



Theses and Dissertations

---

2018-08-01

## An Ecological and Distributional Analysis of Great Basin Bristlecone Pine (*Pinus longaeva*)

Gregory Watson Taylor  
*Brigham Young University*

Follow this and additional works at: <https://scholarsarchive.byu.edu/etd>

---

### BYU ScholarsArchive Citation

Taylor, Gregory Watson, "An Ecological and Distributional Analysis of Great Basin Bristlecone Pine (*Pinus longaeva*)" (2018). *Theses and Dissertations*. 7540.

<https://scholarsarchive.byu.edu/etd/7540>

This Thesis is brought to you for free and open access by BYU ScholarsArchive. It has been accepted for inclusion in Theses and Dissertations by an authorized administrator of BYU ScholarsArchive. For more information, please contact [scholarsarchive@byu.edu](mailto:scholarsarchive@byu.edu), [ellen\\_amatangelo@byu.edu](mailto:ellen_amatangelo@byu.edu).

An Ecological and Distributional Analysis of Great Basin

Bristlecone Pine (*Pinus longaeva*)

Gregory Watson Taylor

A thesis submitted to the faculty of  
Brigham Young University  
in partial fulfillment of the requirements for the degree of

Master of Science

Steven L. Petersen, Chair  
Loreen A. Flinders  
Stanley G. Kitchen

Department of Plant and Wildlife Sciences

Brigham Young University

Copyright © 2018 Gregory Watson Taylor

All Rights Reserved

## ABSTRACT

### An Ecological and Distributional Analysis of Great Basin Bristlecone Pine (*Pinus longaeva*)

Gregory Watson Taylor  
Department of Plant and Wildlife Sciences, BYU  
Master of Science

Understanding the impacts of climate change is critical for improving the conservation and management of ecosystems worldwide. Ecosystems vary along a precipitation and temperature gradient, ranging from tropical jungles to arid deserts. The Great Basin is a semi-arid eco-region that is found within the western United States. Plant communities within the Great Basin range from sagebrush valleys to sub-alpine conifer forests found at high elevation areas. It is predicted that the Great Basin will experience prolonged periods of drought, more intense fires, and greater variability in average annual and monthly precipitation, all in response to changes in climate patterns. At the lower elevations, sagebrush communities are expected to experience less suitable habitat conditions, however, less is understood about vegetation response at upper elevations. Understanding forest composition and structure at these upper elevations within the Great Basin will help us better understand potential impacts from climate change. In chapter 1, we characterized *Pinus longaeva* (Great Basin bristlecone pine D.K. Bailey) forest structure and composition. We mapped this tree species distribution and characterized forest structure and composition using a sampling protocol that included both biophysical variables and individual tree characteristics. We collected data from 69 mixed and homogenous *P. longaeva* stands found within the Great Basin and Colorado Plateau. Results suggest that *P. longaeva* forest structure and composition exhibit high structural variability in tree characteristic measurements like density, basal area, growth rate, age, and in biophysical variables such as substrate type, slope, aspect, elevation, average monthly temperature and precipitation, latitude, and longitude. This study also found that variability in forest composition and structure in *P. longaeva* forests allows for greater flexibility in the breadth of life-history strategies and probable resiliency to climate change. In chapter 2 we used remote sensing images with high spatial resolution to identify 685 unique *P. longaeva* stands on 42 mountain ranges. *Pinus longaeva* was found on the White Mountains on the western edge of the Great Basin to the Colorado Plateau's Henry Mountain and West Tavaputs Plateau in the East, and from the Spring Mountains in the South to the Ruby and Spruce Mountains in the North. Stands covered 113,886 ha across the geographic distribution. A comparison between our maps and those produced by David Charlet found a total of 36% overlap of *P. longaeva*. We mapped 58 unique stands that the control dataset lacked and 11 stands that we did not include. We believe that this is the most comprehensive *P. longaeva* distribution map created to date.

Keywords: Great Basin bristlecone pine, forest ecology, community structure, indicator species, tree growth rate, life-history strategy, Shannon's Diversity Index

## ACKNOWLEDGEMENTS

First, I would like to express my gratitude to my advisor Steve Petersen for his unlimited patience with me as I worked on this thesis. His friendship, reliability, and commitment aided me as I worked through personal challenges and setbacks during the writing process. I would also like to thank Teresa Gomez for her GIS expertise and constant good humor. Her thoughtful reviews provided great insight along the journey. I would like to thank my MS committee members Stan Kitchen, for his excellent mentorship in forest ecology and his help that provided me with improved writing skills, and Loreen Allphin for her help with writing and statistics.

I could not have accomplished this without the support of my family and friends. They encouraged me each step of the way. I would like to personally thank my parents, Gary and Ann Taylor, for their constant support and love.

## TABLE OF CONTENTS

TITLE PAGE .....	i
ABSTRACT .....	ii
ACKNOWLEDGEMENTS .....	iii
TABLE OF CONTENTS .....	iv
LIST OF FIGURES.....	vi
LIST OF TABLES .....	vii
APPENDIX .....	viii
CHAPTER 1.....	1
ABSTRACT .....	1
INTRODUCTION.....	2
METHODS.....	5
Study Design and Plot Selection .....	5
Stand Composition .....	6
Stand Age Structure and Growth Rate .....	7
Tree Species Richness and Diversity .....	8
Data Analysis.....	8
Indicator Species Analysis .....	9
RESULTS.....	9
Indicator Species Analysis .....	11
DISCUSSION .....	12
Stand Composition and Structure:.....	12
CONCLUSIONS.....	15
ACKNOWLEDGMENTS.....	15

LITERATURE CITED .....	16
FIGURES .....	22
TABLES .....	28
APPENDIX .....	30
CHAPTER 2.....	42
ABSTRACT .....	42
INTRODUCTION.....	43
METHODS.....	45
Mapping.....	45
RESULTS.....	47
Mapping.....	47
DISCUSSION .....	48
ACKNOWLEDGMENTS.....	50
LITERATURE CITED .....	52
FIGURES .....	54
TABLES .....	58
APPENDIX.....	59

## LIST OF FIGURES

- Figure 1 - 1. Distribution map showing study plots in the western and eastern Great Basin and Colorado Plateau. Light green points represent Forest Inventory Analysis (FIA) plots and dark blue points represent additional plots. .... 22
- Figure 1 - 2. The boxplots indicate the number of trees per species that occur per plot. .... 23
- Figure 1 - 3. The scatterplot depicts the relationship between tree species richness and elevation across all plots. Tree species richness ranged from 1–7 species ( $r = -0.699$ ). .... 24
- Figure 1 - 4. Scatterplots depict mean age ( $r = 0.263$ ), mean age for PILO ( $r = 0.217$ ), mean growth rate ( $r = 0.089$ ), and mean growth rate for PILO ( $r = 0.105$ ) associations with elevation. Points in each graph represent study plots. Total tree metrics are depicted on the left and *P. longaeva* (PILO) metrics are depicted on the right. .... 25
- Figure 1 - 5. Scatterplots depict basal area ( $r = 0.466$ ), basal area for PILO ( $r = 0.524$ ), and SDI based on basal area ( $r = -0.691$ ) associations with elevation. Points in each graph represent study plots. .... 26
- Figure 1 - 6. Scatterplots depict density ( $r = 0.237$ ), density for PILO ( $r = 0.659$ ), and SDI based on density ( $r = -0.658$ ) associations with elevation. Points in each graph represent study plots. . 27
- Figure 2 - 1. The four distinct geographical sub-regions where *Pinus longaeva* stands were assigned. .... 54
- Figure 2 - 2. Comprehensive *Pinus longaeva* distribution map. Teal polygons represent current *Pinus longaeva* stands. Boxes delineate areas seen at higher resolution in figure 2–2. .... 55
- Figure 2 - 3. Select localities depicting *Pinus longaeva* distribution map. Teal polygons represent current *P. longaeva* stands. .... 56
- Figure 2 - 4. Comparison between the control *Pinus longaeva* distribution map (purple polygons) and our map (teal polygons) at select localities in the state of Nevada. The fire orange polygons demonstrate the areas of overlap between the control distribution and ours. .... 57

## LIST OF TABLES

Table 1 - 1. Average range values for variables measured at each plot as well as mean values for each variable categorized as either homogeneous or heterogeneous. The t-test p-values are expressed from a two-tailed test. \* Represents statistical significance. .... 28

Table 2 - 1. Number of polygons and total hectares found in each of the four *P. Longaeva* sub-regions..... 58



APPENDIX

Table A - 1. List of study plots by ID, name, and geographic location..... 30

Table A - 2. Biophysical variables matrix ..... 33

Table A - 3. Growth Rate Matrix..... 36

Table A - 4. Stand Structure Matrix..... 39

Table A - 5. List of Mountain ranges where *Pinus longaeva* is found across the four sub-regions.  
..... 59

## CHAPTER 1

### *Pinus longaeva* Stand Composition and Structure Reveals Variability within the Ecological Community

Gregory W. Taylor<sup>1</sup>, Stanley G. Kitchen<sup>2</sup>, Loreen Allphin<sup>1</sup>, Steven L. Petersen<sup>1</sup>  
<sup>1</sup>Department of Wildlife Sciences, Brigham Young University, Provo, UT 84602  
<sup>2</sup>US Forest Service, Rocky Mountain Research Station, Provo, UT 84606

#### ABSTRACT

High spatiotemporal variability in forest composition and structure is expected across heterogeneous landscapes. An understanding of this complexity can inform forest practices including improved silvicultural practices, forest conservation, and actions that benefit natural resource policy and preservation of forest resources. Within the Great Basin plant community composition and structure changes across the elevation gradient with salt desert and sagebrush shrubland dominating the lower elevations and sub-alpine forests and alpine tundra dominating the highest elevations. Of these conifers, *Pinus longaeva* D.K. Bailey (Great Basin bristlecone pine) is most often associated with these upper reaches. *Pinus longaeva* is a slow-growing, often long-lived species found in Great Basin and Colorado Plateau forests located in the western USA. Stands that include this conifer exhibit diverse structure and composition in response to variability in abiotic (e.g. precipitation, temperature, substrate, slope, aspect, elevation, fire regime) and biotic (e.g. competition, bark beetle infestation, avian seed dispersers) drivers. The purpose of this study is to characterize the structural and compositional variability within *Pinus longaeva* forested communities. To assess this variation, we analyzed data assembled from 69 forest stands of variable composition with *P. longaeva* present. Stands were representative of the full geographic and elevational range of the species. Plot sampling and data processing protocols followed those developed by the USFS, Forest Inventory and Analysis program and included

measurement or estimation of biophysical, stand and individual tree characteristics. We calculated average growth rate, tree species richness and Shannon-Wiener's diversity indices (based upon tree density and basal area) for each plot. Stands ranged in elevation from 2179 to 3476 m and included one to seven tree species per stand. *Pinus longaeva* dominated stands at higher elevations, while stand composition at lower elevations was more heterogeneous. At lower elevations, *P. longaeva* stands were more commonly found on northeast slopes, while at higher elevations there was no correlation to aspect. Density and live tree basal area for *P. longaeva* increased with elevation up to approximately 3250 m. Indicator species analysis found that *Abies concolor* appeared 50% of the time in plots where *P. longaeva* was present, compared to aspen which was present only 2%. Observed variability in forest composition and structure across an elevational gradient may indicate greater flexibility in *P. longaeva* life-history strategy than has been previously reported.

## INTRODUCTION

Forested ecosystems provide critical ecosystem services including sustainable hydrological cycling (Salati 1987, Lexer et al. 2002), protection against erosion (Hartanto et al. 2003), nitrogen cycling (Spies and Franklin 1991), carbon fixation, oxygen production (Schimel 1995), critical habitat for numerous flora and fauna species (Tews et al. 2004), food and fiber resources (Ogle 1996, Johns 1997), unique chemical compounds used in current medicines (Abelson 1990), and places of natural beauty and wonder for human recreation (Prideaux 2015). The specific capacity of forest communities to sustain desirable ecological outcomes in the presence of natural and human-caused disturbance is intrinsically tied to composition and structure at the stand scale. In its simplest form, stand composition is a measure of the cumulative contributions or relative abundances of tree species in all life-history stages while

stand structure varies with density, size, age, and spatial arrangement of individual trees (McElhinny et al. 2005). Characterization of the ecological processes and factors that influence compositional and structural variability provide a platform from which to assess risk to naturally occurring forest systems and the benefits that they provide (Lexer et al. 2002). As climate change occurs resulting in prolonged periods of drought (Dai 2012), increased wildfire intensity (Westerling et al. 2006), and an increase in summer precipitation and decrease in winter precipitation (Barnett et al. 2005, Trenberth 2011) it will become important to understand the composition and structure of different landscapes across the world—specifically forests. Here we focus on the *Pinus longaeva* D.K. Bailey (Great Basin bristlecone pine) forests of the Great Basin. Prolonged periods of drought in the Great Basin may make certain trees within *P. longaeva* forests more susceptible to pine beetles, white pine blister rust, and wildfire (Allen et al. 2010). As fuel loads (desiccated trees) increase, wildfire intensity also increases, which could result in structural changes in *P. longaeva* forests. Climate change may also extend the growing seasons at higher elevations resulting in increased inter-species competition within *P. longaeva* forests (Davis and Shaw 2001, Walther et al. 2002).

*Pinus longaeva* forests are scattered across the central and southern Great Basin and portions of the Colorado Plateau, ranging in elevation from 2,200 to 3,500 m (Hiebert and Hamrick 1984). The climate for the region is semiarid continental with temperatures decreasing and precipitation increasing with elevation (Peterson, 1994). Precipitation comes in the form of cold-season (October–May) snow or rain and monsoonal rains in summer months (June–August). In its range, *P. longaeva* is subject to harsh environmental conditions that include low temperatures, desiccating winds, low soil water retention capacity, and high soil erosion potential (LaMarche 1969, Lanner 2002). *Pinus longaeva* grows predominately in rocky dolomitic and limestone based soils (LaMarche 1969, Beasley and Klemmedson 1980); however, stands have

been documented growing in mixed alluvium, basalt, chert, granite, Precambrian schist, quartzite, rhyolite, siltstone, and sandstone derived soils (Nelson 1976, Charlet 2015, Orlemann 2017).

Bailey (1970) provided the first detailed life history, genetic, and morphological descriptions for this species, describing the species as “erect trees showing pendulous and twisting branching”. He noted that *P. longaeva* trees are most commonly found on limestone or dolomite substrates in the Great Basin. Additionally, he found that *P. longaeva* is temperature sensitive at high elevations (a shorter growing season at upper tree-line) and precipitation dependent at lower elevations. Other studies on *P. longaeva* provide additional insight into their general ecology and geographic distribution. Past research has identified high genetic heterozygosity within stands, but low heterozygosity between stands based upon evaluation of a limited number of stands in eastern Nevada and western Utah (LaMarche 1969, 1973). Results were interpreted as indicative of high levels of gene flow among stands over time (Hiebert and Hamrick 1984). Research by LaMarche (1969, 1973) focused primarily on tree ages and recruitment in high-elevation stands located in the White Mountains of California (particularly the Schulman grove). Further research characterized *P. longaeva* tree ages and growth patterns in relation to environmental conditions for two stands in eastern Nevada (Beasley and Klemmedson 1980).

Despite focused research conducted on limited stands and with sizeable portions of the distribution mapped, there remains large gaps in our understanding of *P. longaeva* stand composition and structure and species distribution. For example, little is known about the age structure, growth rates, and community composition at the lowest elevations where *P. longaeva* occurs. Additionally, comparisons of community composition and structure across the entire *P. longaeva* distribution do not exist.

The purpose of this study is to (1) characterize variability in *P. longaeva* stand composition and structure in its known geographic and ecological (elevational) distributions, (2) identify patterns of stand variability that might be linked to ecological function and (3) ascertain abiotic drivers responsible for regulating stand dynamics in bristlecone pine forests. We address these objectives by (1) quantifying *P. longaeva* community composition (abundances and diversity of all tree species) and structure (density, basal area, and age/size structure) for a series of sites representative of the full species range, (2) employing the use of correlation analysis that facilitates identification of non-random patterns among traits across all sites, and (3) assessing the influence of abiotic drivers (i.e. precipitation, substrate type, temperature, elevation, slope, aspect) on tree and stand traits across the study area. We hypothesized that there would be substantial stand-level differences in composition and structure, and that the differences would be predictable and follow biophysical gradients. Our null hypothesis was that there would be no differences between *P. longaeva* forest structure and composition across its geographic distribution, or that differences would be manifest independent of the biophysical environment. If supported, our hypothesis could indicate the evolution of a plastic life-history strategy that has allowed this species to exist across a broad range of environmental conditions. Flexibility in life-history strategy may in turn provide needed resiliency to environmental stressors such as climate change, novel pathogens, and bark beetle outbreaks (Miller et al. 2017).

## METHODS

### *Study Design and Plot Selection*

The USDA Forest Service Inventory and Analysis (FIA) Program utilizes a systematic network of thousands of permanently-located plots (326,247 plots in 2015) and standardized

forest mensuration protocols to produce comprehensive assessments of forest condition and trend across the conterminous United States (Vogt and Smith 2016). We acquired data for the 51 plots from the Great Basin and Colorado Plateau ecoregions in which *P. longaeva* trees were present (Figure 1-1). We augmented these data by establishing an additional 18 plots using FIA protocols in forested locations known to include *P. longaeva*. For these plots, study stands were selected to represent the full geographic and elevational range (2179-3456 m) of the species. Coordinates were randomly pre-selected from within boundaries of targeted forest stands and located in the field using hand-held GPS devices. The combination of traditional FIA plots and our additional, targeted plots provide data for a total of 69 distinct and representative *P. longaeva* forest communities (Table A-1).

Study plots included four circular subplots (radius 7.32 m), one of which is positioned at the plot center and the other three centered at a horizontal distance of 36.58 m from plot center at bearings of 0°, 120°, 240°. We estimated slope, aspect, and elevation for each subplot. (Hijmans et al. 2005).

### *Stand Composition*

Within each subplot, distance and azimuth from subplot center was measured for all living and standing dead trees with diameters at breast height (DBH; 1.4 m above ground level; side slope position) that exceeded 2.54 cm. Trees with separate pith at ground level were treated as separate trees (Woudenberg et al. 2010). Tree density (trees/ha) was calculated by species and for all species combined by multiplying the sum of trees in the four subplots by 14.88. Tree length (height) was estimated and DBH measured using calipers or a metric steel diameter tape. We calculated individual tree basal area (Husch et al. 2003), summed values by plot and converted results to m<sup>2</sup>/ha. We measured a total of 2324 trees of which 925 (40%) were *P.*

*longaeva* and the remainder assigned to 12 other species. Eighty-four percent (1947) of measured trees were alive.

### *Stand Age Structure and Growth Rate*

We extracted cores from 1,210 trees located in our 18 supplemental plots using standard three-thread increment borers. Coring was attempted for most living trees (very small conifers and non-conifers were not included) and some snags with solid wood for 14 of the 18 plots. We selected representative trees by size class for the other four plots. Small conifer age estimates were made by counting sets of branch whorls. We extracted core samples at 20-100 cm above side-slope ground level and cored up to four times per tree in order to obtain a sample as close to tree center (pith) as possible. For multi-branched sets of trees that appeared to have a common origin (single seed cache), we attempted to obtain a datable core from a single tree and assumed a common age for the group. Tree cores were labeled and stored in paper tubes for protection during transportation from the field to the laboratory. For the 51 FIA plots, we used age estimates developed by FIA crews. For these plots, aged trees were meant to be representative of the size classes present and the proportion of trees with assigned ages varied among plots.

We glued tree cores onto mounts, and sanded surfaces with increasingly fine sand paper until cell and ring structure were clearly visible using a binocular microscope (15-75 power). Tree cores were cross-dated using locally-developed annual ring-width chronologies and lists of marker (narrow) rings (Stokes and Smiley 1968) to determine the year associated with the pith or inner-most ring. For samples missing pith, age was estimated by matching ring curvature and spacing to concentric rings in a transparent overlay and adjusting for missing rings (Applequist 1958). We treated pith dates as conservative estimates of establishment dates, employing no correction factors because of unknown and variable time lapses between germination and the



year trees reached core height. We calculated growth rate (cm/yr) for each tree with an estimated age by dividing diameter by tree age.

### *Tree Species Richness and Diversity*

The number of species per plot (four subplots) were summed to assess tree species richness (1-7). Plots were arbitrarily defined with 1-3 tree species as homogeneous plots and plots with  $\geq 4$  tree species as heterogeneous. We calculated separate Shannon-Wiener Diversity Indices (SDIs) based on tree species density and BA values for each site using the following equation:

$$H' = -\sum_{i=1}^S (p_i \ln p_i)$$

where  $p_i$  represents the proportion of individuals of one particular species found divided by the total number of individuals found,  $S$  represents the number of species in the sample, and  $H'$  represents the Shannon-Wiener diversity index (Pielou 1975).

The Shannon-Wiener Diversity Index characterizes species diversity in a community by accounting for both abundance and evenness of the species present (Shannon 2013).

### *Data Analysis*

To determine correlation significance of plot structure and composition values with biophysical characteristics of the environment, we constructed matrices using stand composition, stand structure, and stand environmental variables (Tables A-2 to A-4). A square-root transformation was applied to BA and density (all species combined and bristlecone pine only)

values to normalize and reduce the variance in the dataset. In order to adjust for the circular nature of the aspect angle, a trigonometric transformation was applied (Beers et al. 1966). Both sine and cosine transformations were used, but in every case, only one transformation was needed to explain the variable's contribution to the analysis. This is because cosine is simply a functional transformation of sine. Without loss of generality, sine was chosen.

### *Indicator Species Analysis*

An Indicator Species Analysis (ISA) model was used to identify the strength of association between *P. longaeva* and other tree species using PC-ORD version 6.0 (McCune and Mefford 2011). Indicator Species Analysis (ISA) assesses the degree to which a particular species characterizes a group based on its abundance in the sample units (Peck 2010). It provides an indicator value (IV) which marks the relative abundance and constancy within each group of that species. The higher the value the more abundant and constant that species is in the forest stand. This value is determined by multiplying the relative species frequency by that species relative abundance. We analyzed the quantitative species abundance dataset using the Dufrene and Legendre analysis option (Dufrene and Legendre 1997). We selected the randomization option and used the time of day as the random number seed. No IV values under 20.0 or with an alpha level  $< .02$  were considered significant (Dufrene and Legendre 1997).

## RESULTS

*Pinus longaeva* was found growing in both homogeneous and heterogeneous stands across the range of the species. We classified, 37 plots and associated stands as homogeneous (1-3 species) and 32 as heterogeneous ( $\geq 4$  species). Tree species recorded within the plots included

*Abies concolor* Gord. & Glend. (white fir), *Abies lasiocarpa* Hook. (subalpine fir), *Cercocarpus ledifolius* Nutt. (curl-leaf mountain mohogany), *Juniperus osteosperma* Torr. (Utah juniper), *Juniperus scopulorum* Sarg. (Rocky Mountain juniper), *Picea engelmannii* Parry (Engelmann spruce), *Pinus edulis* Engelm. (twin-needle pinyon), *Pinus flexilis* James (limber pine), *Pinus longaeva*, *Pinus monophylla* Torr. & Frem. (single-leaf pinyon), *Pinus ponderosa* Dougl. (ponderosa pine), *Populus tremuloides* Michx. (quaking aspen), and *Pseudotsuga menziesii* Mirb. (Douglas fir) (Figure 1-2). The more dominant species occurring with *P. longaeva* include *A. concolor*, *C. ledifolius*, *P. flexilis*, and *P. menziesii*, however this varied across the plots. Tree species richness within our plots ranged from one (11 plots) to seven tree species (2 plots), however, study plots with more than five species (6 plots) were uncommon (Figure 1-3).

Variables associated with stand composition and structure varied by orders of magnitude among plots (Table 1-1). Mean values for homogeneous and heterogeneous plots differed substantially for most structural traits.

Of all the biophysical variables examined, elevation demonstrated stronger correlations with measured and calculated stand variables (Figures 1-4 to 1-6). Comparisons between mean live tree age ( $r = 0.263$ ,  $p = 0.0332$ ), mean live tree growth rates ( $r = 0.089$ ,  $p = 0.4620$ ), *P. longaeva* live tree age ( $r = 0.217$ ,  $p = 0.0887$ ), and *P. longaeva* growth rates ( $r = 0.105$ ,  $p = 0.4142$ ) with elevation do not demonstrate any significant relationship, besides mean live tree age (Figure 1-4a-d). Total basal area for all trees ( $r = 0.466$ ,  $p < 0.0001$ ) and for *P. longaeva* trees ( $r = 0.524$ ,  $p < 0.0001$ ) exhibited significant correlations with elevation (Figure 1-5a, b). Density for all trees combined varied independent of elevation ( $r = 0.237$ ,  $p = 0.0497$ ), however density for *P. longaeva* trees was significantly and positively correlated with elevation ( $r = 0.659$ ,  $p < 0.0001$ ) (Figure 1-6a, b). Tree species richness ( $r = 0.699$ ,  $p < 0.0001$ ) (Figure 1-2) and all measures of stand diversity (SDI; based upon total live tree basal area ( $r = -0.691$ ,  $p < 0.0001$ ))

(Figure 1-5c) and based upon total live tree density ( $r = -0.658$ ,  $p < 0.0001$ ) (Figure 1-6c), were inversely correlated with elevation.

Homogeneous and heterogeneous plot comparisons demonstrate differences and similarities across plot variables (Table 1-1). These comparisons demonstrate statistically significant differences ( $p < 0.05$ ) between elevation, tree diameter, PILO tree diameter, plot tree basal area, PILO plot tree basal area, PILO plot tree density, plot SDI based on basal area, and plot SDI based on density.

### *Indicator Species Analysis*

*Abies concolor* (IV=56.3;  $p < 0.0000$ ) and *P. tremuloides* (IV=16.7;  $p = 0.0504$ ) received the highest indicator values in the analysis, however only *A. concolor* was predictive of *P. longaeva* plots. *Abies concolor* appeared in 35 of 69 plots, whereas *P. tremuloides* only appeared in 2 of the 69 plots. This suggests that there is a 50% probability that where *P. longaeva* is *A. concolor* will also be present, and that where *P. longaeva* is *P. tremuloides* will most likely not be present. This analysis was independent of plot type (homogeneous vs heterogeneous). The other ten species expressed low indicator values that suggest that they do not appear with higher levels of certainty in *P. longaeva* plots. We did see that *A. concolor*, *A. lasiocarpa*, *P. engelmanni*, *P. flexilis*, *P. longaeva*, and *P. menzeiseii* occurred more frequently in the homogeneous plots, while *C. ledifolius*, *J. osteosperma*, *J. scopulorum*, *P. edulis*, *P. monophylla*, *P. tremuloides* and *P. ponderosa* were found more frequently in the heterogeneous plots.

## DISCUSSION

### *Stand Composition and Structure:*

The results of this study found that *P. longaeva* forest plots are highly variable in composition and structure across the geographic and elevational range of the species. The high variability of forest composition and structure in *P. longaeva* stands is likely due to variations among biophysical variables (Salzer et al. 2009). A previous study by Hiebert and Hamrick (1984) supports our findings that tree species richness in our plots varied from five to seven species at lower elevations, while upper elevations had less than four species present. As the ISA showed that *A. concolor* was frequently present in our plots, a study by Guisan et al. (1999) found that *A. concolor* occurs at mid-elevation plots abundantly in the southern Great Basin. *Populus tremuloides* does not appear often in plots where *P. longaeva* is present because it prefers deeper soils found on a slope or on a depression where water accumulates. *Populus tremuloides* are for the most part water dependent plants, so they mostly grow in areas with greater soil water availability (Weigle and Frothingham 1911). *Pinus longaeva* grows in areas that most likely will go through a drying experience that aspen do not tolerate well.

Previous studies show that there is a correlation between age and elevation; however, these studies were based on three to four *P. longaeva* localities that are known for their old-aged trees (LaMarche 1969, LaMarche and Mooney 1972, LaMarche 1973, Hiebert and Hamrick 1984). We found that age was not significantly correlated with elevation, but rather mean tree age varied independent of elevation. This proved true for plots where just *P. longaeva* age was compared across elevations as well. Our study presents a representation of the entire *P. longaeva* forest distribution in which we compare tree diameter and age across a wide range of elevation, which are direct factors for determining growth rate. While Salzer et al. (2009) describes varied

growth rates at higher *P. longaeva* elevation plots, we also found variation among growth rates across the elevation gradient. Stevens (1992) also found that increases in elevation directly correlates with a decrease in tree species richness of forests in general.

Our results are similar to that of Salzer et al. (2009) in that *P. longaeva*-dominant stands were more homogeneous, tree ages were generally older, and basal areas and densities were larger (Tables A-3 and A-4) than heterogeneous plots with *P. longaeva* present but not a dominate species. It is important to note that Hiebert and Hamrick (1984) found that population densities were highest at the lower elevations in their plots, whereas we found plot density levels (all trees combined) varied an elevation gradient Figure 6a).

Weisberg and Baker (1995) suggest that soil moisture and microclimatic conditions at higher elevations are more suitable to tree seed germination and establishment, likely due to higher precipitation levels, cooler air and soil temperatures, and lower evapotranspiration rates. Although precipitation is generally greater with increasing elevation, shallow soils typical of upper tree line locations experience lower soil water infiltration rates that can limit seedling growth for tree species (Kupfer and Cairns 1996, Sveinbjörnsson 2000), however in our study we found *A. lasiocarpa*, *A. concolor*, *P. engelmanni*, *P. flexilis*, *P. longaeva*, and *P. menzeiseii* present at higher elevations, thus suggesting that while the effects of shallow soils may deter some species from growing, it did not affect all. We also found *P. longaeva* at high elevation plots growing more often on north-eastern aspects and moderate to steep slopes. This is because those aspects have slower evaporation and likely evapotranspiration rates which result in plants having greater soil water availability. This leads to greater plant productivity, higher organics, and higher nutrient availability, which result in deeper soils due to water and weathering potential as well as greater root development. Additionally, higher elevations experience shorter

growing seasons, which may prevent other tree species that need a longer growing season from competing with *P. longaeva*.

Previous research has demonstrated that *P. longaeva* exhibits low shade tolerance (Bailey 1970). Interestingly, we observed the effects of shade on tree and stand development. One would expect that where there is competition for light – whether between species or within – density of *P. longaeva* would be affected. In fact, at lower elevations where the stands were more heterogeneous, *P. longaeva* was dominated by other species. In more homogenous stands, although the trees are stronger due to a reduction in interspecies competition, they still distribute more sparsely indicating that they compete with each other for light. Other factors driving competition for space include: aspect, slope, soil type, soil depth, water availability, and climatic conditions. Interestingly, at the heterogeneous plots we found that aspect served as a better indicator of *P. longaeva* distribution where suitable site conditions are more limited. Specific to these areas, rock substrate was a good indicator of stand locations. Petersen et al. (2004) found that rocks provide microsite conditions that improve soil moisture retention and decreased evapotranspiration rates resulting in higher establishment compared to non-rocky plots. Sampled *P. longaeva* trees were consistently found growing on dolomitic sandstone and limestone soil substrates (Wright and Mooney 1965). In areas with low soil water retention capacity porous limestone and sandstone enable greater water retention compared to granitic or volcanic substrate types common within the Great Basin (Estrada-Medina et al. 2010, Estrada-Medina et al. 2013). These highly porous soils allow for deeper root penetration and establishment, which enhances tree growth in difficult physical and environmental conditions (Schoonover and Crim 2015).

## CONCLUSIONS

Our study is the first to compare *P. longaeva* forest composition and structure from biophysical variables across the known geographic distribution. This qualitative analysis indicates that plots vary in structure and composition in the geographic distribution and across elevational gradients. We predict that flexibility in the breadth of life-history strategies allows for greater variability in forest composition and structure in *P. longaeva* stands. Our analyses demonstrate that *P. longaeva* has adapted to a wide variety of environmental conditions and maintained sexually viable stands over time. The results show that *P. longaeva* stand composition and structure varies in its geographic distribution (western Colorado Plateau, southern and central Great Basin). This flexibility in breadth of life-history strategies we hypothesize increases the tree's fitness, prolongs its longevity, and enhances its resilience to potentially harmful factors like climate change. A better understanding of *P. longaeva* forest composition and structure provides a foundation from which to assess the specific capacity of these forests to sustaining desirable ecological outcomes in the future.

## ACKNOWLEDGMENTS

This project was partially funded by a grant from the USDA Forest Service, Western Wildland Environmental Threat Assessment Center and the Rocky Mountain Research Station (RJVA-14-JV-11221632-099). Additional funding was also provided by Brigham Young University, Charles Redd Foundation Center for Western Studies. We appreciate the support and resources provided by the Brigham Young University Geospatial Habitat Analysis Laboratory. We especially thank Teresa Gomez for her valuable input and reviews. We thank Chris Balzotti for assistance in data collection.



## LITERATURE CITED

- Abelson, P. H. 1990. Medicine from plants. *Science* 247:513-514.
- Allen, C. D., A. K. Macalady, H. Chenchouni, D. Bachelet, N. McDowell, M. Vennetier, T. Kitzberger, A. Rigling, D. D. Breshears, E. H. Hogg, P. Gonzalez, R. Fensham, Z. Zhang, J. Castro, N. Demidova, J.-H. Lim, G. Allard, S. W. Running, A. Semerci, and N. Cobb. 2010. A global overview of drought and heat-induced tree mortality reveals emerging climate change risks for forests. *Forest Ecology and Management* 259:660-684.
- Applequist, M. 1958. A simple pith locator for use with off-center increment cores. *Journal of Forestry*. Bailey, D. K. 1970. Phylogeography and taxonomy of pinus subsection Balfourianae. *Annals of the Missouri Botanical Garden* 57:210-249.
- Barnett, T. P., J. C. Adam, and D. P. Lettenmaier. 2005. Potential impacts of a warming climate on water availability in snow-dominated regions. *Nature* 438:303.
- Beasley, R. S., and J. O. Klemmedson. 1980. Ecological relationships of bristlecone pine. *The American Midland Naturalist* 104:242-252.
- Beers, T. W., P. E. Dress, and L. C. Wensel. 1966. Notes and observations: Aspect transformation in site productivity Research. *Journal of Forestry* 64:691-692.
- Charlet, D. A. 2015. Atlas of Nevada conifers: a phylogeographic reference. Second edition. University of Nevada Press, Reno, NV. Unpublished data.
- Dai, A. 2012. Increasing drought under global warming in observations and models. *Nature Climate Change* 3:52.
- Davis, M. B., and R. G. Shaw. 2001. Range shifts and adaptive responses to quaternary climate change. *Science* 292:673-679.
- Dufrene, M., and P. Legendre. 1997. Species assemblages and indicator species: the need for a flexible asymmetrical approach. *Ecological monographs* 67:345-366.

- Estrada-Medina, H., W. Tuttle, R. C. Graham, M. F. Allen, and J. J. Jiménez-Osornio. 2010. Identification of underground karst features using ground-penetrating radar in Northern Yucatán, México. *Vadose Zone Journal* 9:653-661.
- Estrada-Medina, Hector, R. C. Graham, M. F. Allen, J. J. Jimenez-Osornio, and S. Robles-Casolco. 2013. The importance of limestone bedrock and dissolution karst features on tree root distribution in northern Yucatan, Mexico. *Plant and Soil* 362:37-50.
- Guisan, A., S. B. Weiss, and A. D. Weiss. 1999. GLM versus CCA spatial modeling of plant species distribution. *Plant Ecology* 143:107-122.
- Hartanto, H., R. Prabhu, A. S. Widayat, and C. Asdak. 2003. Factors affecting runoff and soil erosion: plot-level soil loss monitoring for assessing sustainability of forest management. *Forest Ecology and Management* 180:361-374.
- Hiebert, R. D., and J. L. Hamrick. 1984. An ecological study of bristlecone pine (*Pinus longaeva*) in Utah and Eastern Nevada. *Great Basin Naturalist* 44:487-494.
- Hijmans, R. J., S. E. Cameron, J. L. Parra, P. G. Jones, and A. Jarvis. 2005. Very high resolution interpolated climate surfaces for global land areas. *International journal of climatology* 25:1965-1978.
- Husch, B., T. W. Beers, and J. A. Kershaw. 2003. *Forest mensuration*. 4th edition. John Wiley & Sons, Inc. , Hoboken, New Jersey.
- Johns, A. G. 1997. *Timber production and biodiversity conservation in tropical rain forests*. Cambridge University Press.
- Kupfer, J. A., and D. M. Cairns. 1996. The suitability of montane ecotones as indicators of global climatic change. *Progress in Physical Geography* 20:253-272.
- LaMarche, V. C. 1969. Environment in relation to age of bristlecone pines. *Ecology* 50:53-59.

- LaMarche, V. C. 1973. Holocene climatic variations inferred from treeline fluctuations in the White Mountains, California. *Quaternary Research* 3:632-660.
- LaMarche, V. C., and H. A. Mooney. 1972. Recent climatic change and development of the bristlecone pine (*P. longaeva* Bailey) krummholz zone, Mt. Washington, Nevada. *Arctic and Alpine Research* 4:61-72.
- Lanner, R. M. 2002. Why do trees live so long? *Aging Research Reviews* 1:653-671.
- Lexer, M. J., K. Hönninger, H. Scheifinger, C. Matulla, N. Groll, H. Kromp-Kolb, K. Schadauer, F. Starlinger, and M. Englisch. 2002. The sensitivity of Austrian forests to scenarios of climatic change: a large-scale risk assessment based on a modified gap model and forest inventory data. *Forest Ecology and Management* 162:53-72.
- McCune, B., and M. J. Mefford. 2011. PC-ORD. Multivariate analysis of ecological data. . MjM Software, Gleneden Beach, Oregon, U.S.A.
- McElhinny, C., P. Gibbons, C. Brack, and J. Bauhus. 2005. Forest and woodland stand structural complexity: Its definition and measurement. *Forest Ecology and Management* 218:1-24.
- Miller, S., A. Schoettle, K. Burns, R. Snieszko, and P. Champ. 2017. Preempting the pathogen: Blister rust and proactive management of high-elevation pines. *Science You Can Use Bulletin*:11.
- Nelson, M. G. 1976. The montane coniferous forests of the northern Deep Creek Range, Utah. Unpublished thesis, University of Utah, Salt Lake City:73.
- Ogle, B. 1996. People's dependency on forests for food security. *Current issues in non-timber forest products research*:219-242.
- Orlemann, A., Flinders, Steven H., Allphin, Loreen. 2017. The discovery of Great Basin bristlecone pine, *Pinus longaeva*, in the Tushar Mountains of the Fishlake National Forest in Central Utah, USA. *Western North American Naturalist* 77:7.

- Peck, J. E. 2010. Multivariate analysis for community ecologists: step-by-step using PC-ORD. MjM Software Design, Gleneden Beach, Or.
- Petersen, S. L., B. A. Roundy, and R. M. Bryant. 2004. Revegetation methods for high-elevation roadsides at Bryce Canyon National Park, Utah. *Restoration Ecology* 12:248-257.
- Peterson, F. 1994. Sand dunes, sabkhas, streams, and shallow seas: Jurassic paleogeography in the southern part of the western interior basin. *Mesozoic Systems of the Rocky Mountain Region*:233-272.
- Pielou, E. C. 1975. *Ecological diversity*. Wiley Interscience, New York.
- Prideaux, B. 2015. *Recreation in forests*.
- Salati, E. 1987. *The forest and the hydrological cycle*.
- Salzer, M. W., M. K. Hughes, A. G. Bunn, and K. F. Kipfmueller. 2009. Recent unprecedented tree-ring growth in bristlecone pine at the highest elevations and possible causes. *Proceedings of the National Academy of Sciences* 106:20348-20353.
- Schimel, D. S. 1995. Terrestrial ecosystems and the carbon cycle. *Global Change Biology* 1:77-91.
- Schoonover, J. E., and J. F. Crim. 2015. An introduction to soil concepts and the role of soils in watershed management. *Journal of Contemporary Water Research & Education* 154:21-47.
- Shannon, C. E. 2013. A mathematical theory of communication. *Bell System Technical Journal* 27:379-423.
- Spies, T. A., and J. F. Franklin. 1991. The structure of natural young, mature, and old-growth douglas-fir forests in Oregon and Washington. *Wildlife and vegetation of unmanaged Douglas-fir forests*: 91-109.

- Stevens, G. C. 1992. The elevational gradient in altitudinal range: an extension of rapoport's latitudinal rule to altitude. *The American Naturalist* 140:893-911.
- Sveinbjörnsson, B. 2000. North American and European treelines: External forces and internal processes controlling position. *AMBIO: A Journal of the Human Environment* 29:388-395.
- Tews, J., U. Brose, V. Grimm, K. Tielbörger, M. Wichmann, M. Schwager, and F. Jeltsch. 2004. Animal species diversity driven by habitat heterogeneity/diversity: the importance of keystone structures. *Journal of Biogeography* 31:79-92.
- Trenberth, K. E. 2011. Changes in precipitation with climate change. *Climate Research* 47:123-138.
- Vogt, J. T., and W. B. Smith. 2016. Forest inventory and analysis fiscal year 2015 business report. United States Department of Agriculture, USA.
- Walther, G.-R., E. Post, P. Convey, and A. Menzel. 2002. Ecological responses to recent climate change. *Nature* 416:389.
- Weisberg, P. J., and W. L. Baker. 1995. Spatial variation in tree seedling and krummholz Growth in the forest-tundra ecotone of Rocky Mountain National Park, Colorado, U.S.A. *Arctic and Alpine Research* 27:116-129.
- Westerling, A. L., H. G. Hidalgo, D. R. Cayan, and T. W. Swetnam. 2006. Warming and earlier spring increase Western U.S. forest wildfire activity. *Science* 313:940-943.
- Woudenberg, Sharon W., Conkling, Barbara L., O'Connell, Barbara M., LaPoint, Elizabeth B., Turner, Jeffery A., Waddell, Karen L. 2010. The forest Inventory and analysis database: database description and users manual version 4.0 for Phase 2. Gen. Tech. Rep. RMRS-GTR-245. Fort Collins, CO: U.S. Department of Agriculture, Forest Service, Rocky Mountain Research Station.

Wright, R. D., and H. A. Mooney. 1965. Substrate-oriented distribution of bristlecone pine in the White Mountains of California. *The American Midland Naturalist* 73:257-284.

## FIGURES

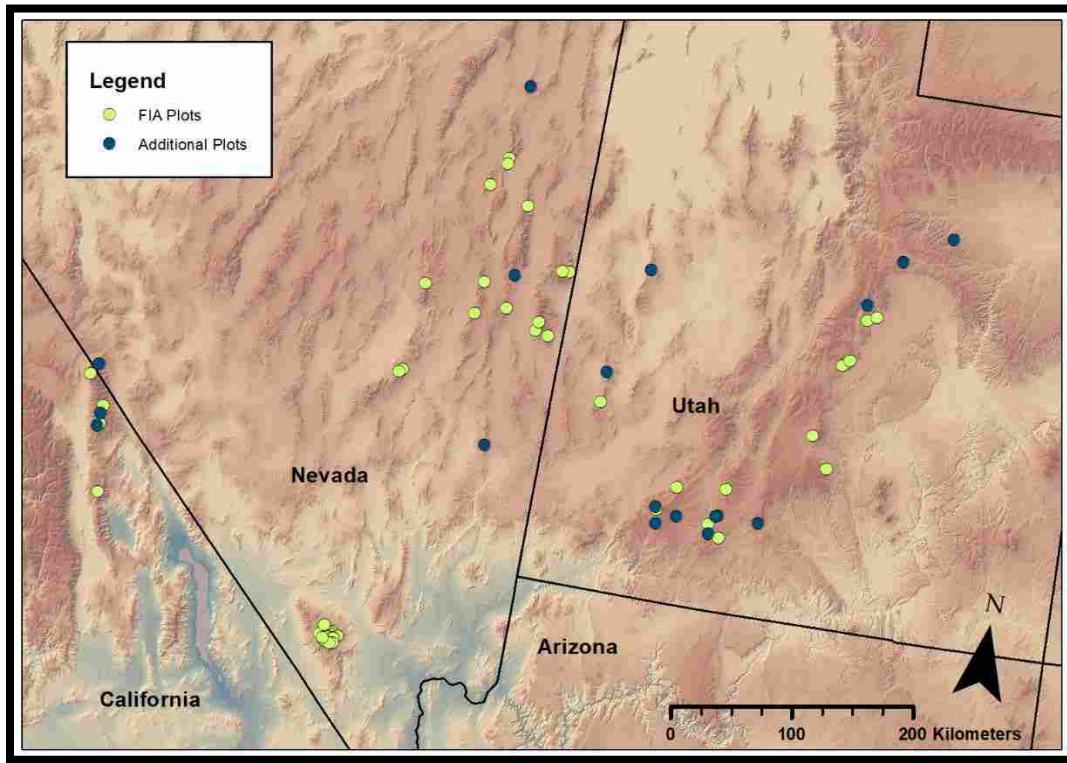


Figure 1 - 1. Distribution map showing study plots in the western and eastern Great Basin and Colorado Plateau. Light green points represent Forest Inventory Analysis (FIA) plots and dark blue points represent additional plots.

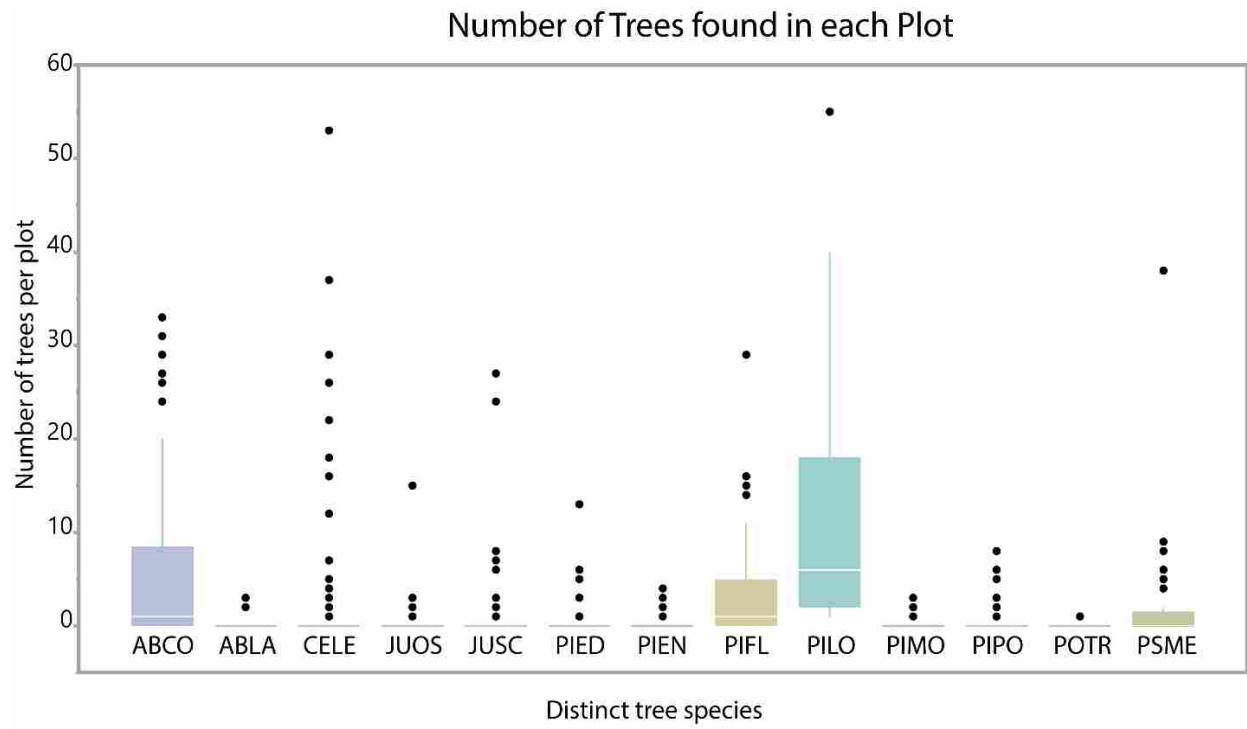


Figure 1 - 2. The boxplots indicate the number of trees per species that occur per plot.



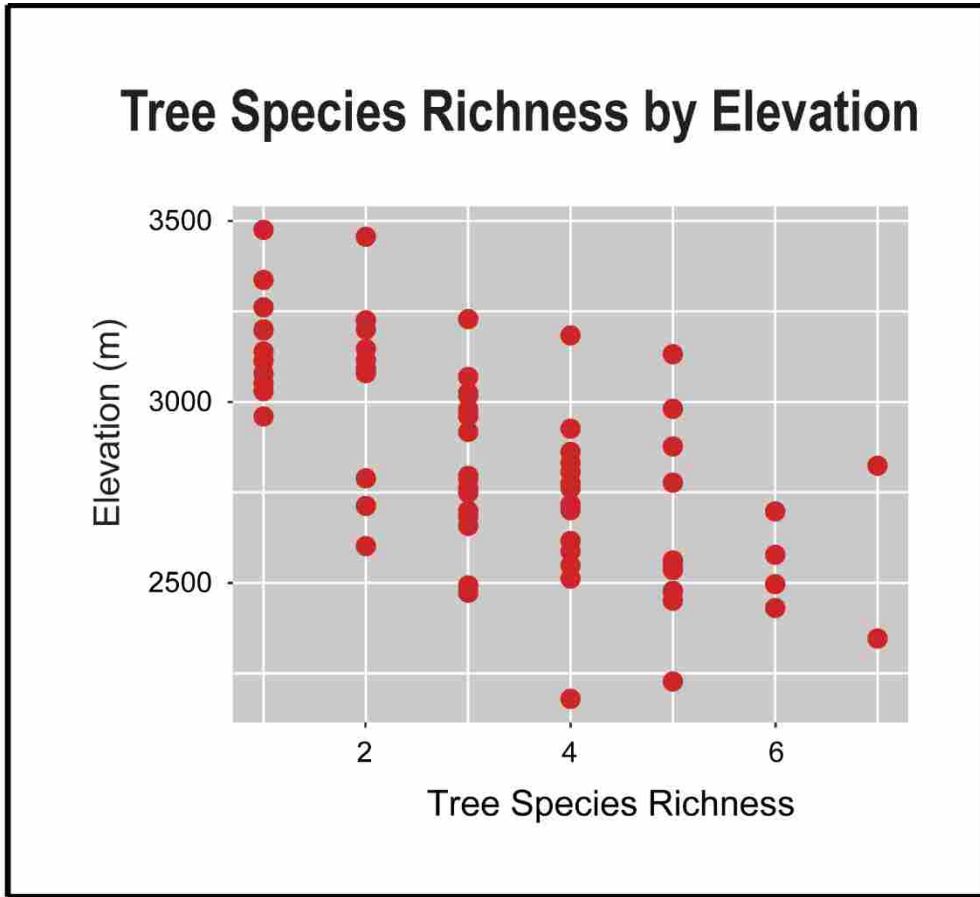


Figure 1 - 3. The scatterplot depicts the relationship between tree species richness and elevation across all plots. Tree species richness ranged from 1–7 species ( $r = -0.699$ ).

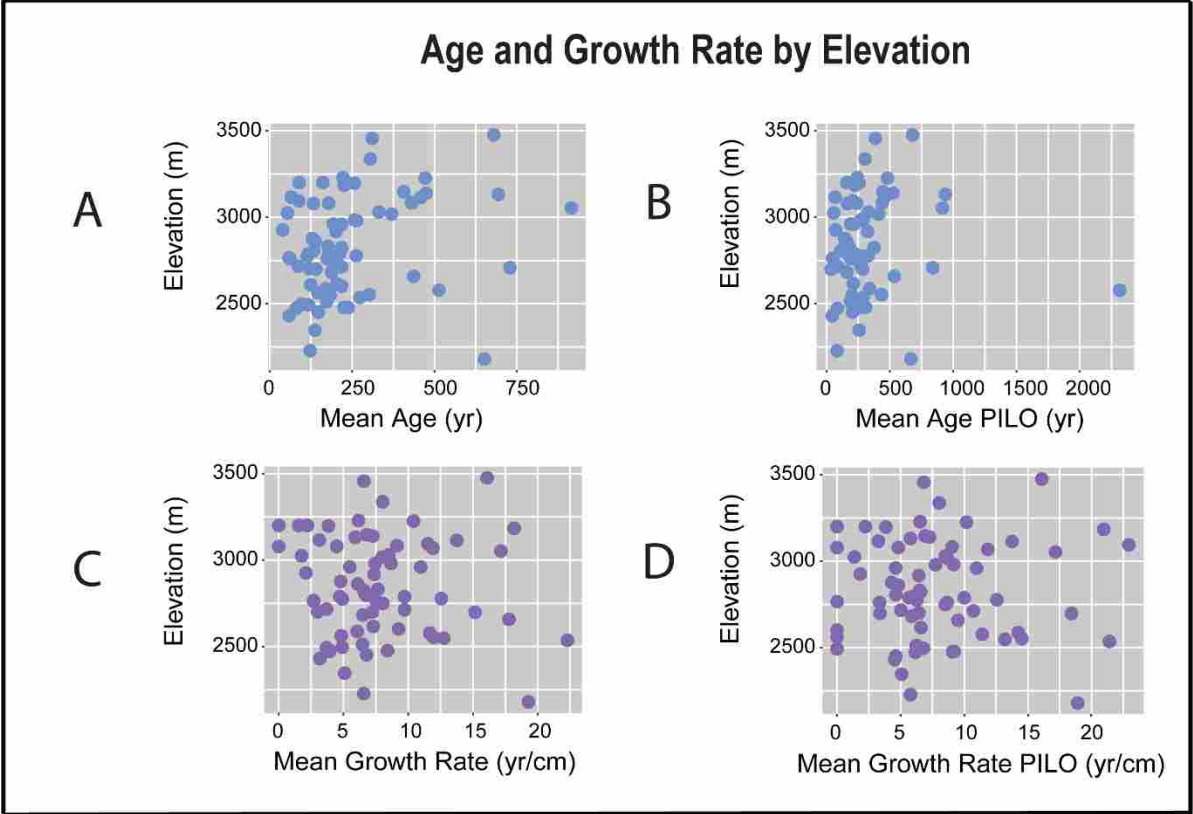


Figure 1 - 4. Scatterplots depict mean age ( $r = 0.263$ ), mean age for PILO ( $r = 0.217$ ), mean growth rate ( $r = 0.089$ ), and mean growth rate for PILO ( $r = 0.105$ ) associations with elevation. Points in each graph represent study plots. Total tree metrics are depicted on the left and *P. longaeva* (PILO) metrics are depicted on the right.

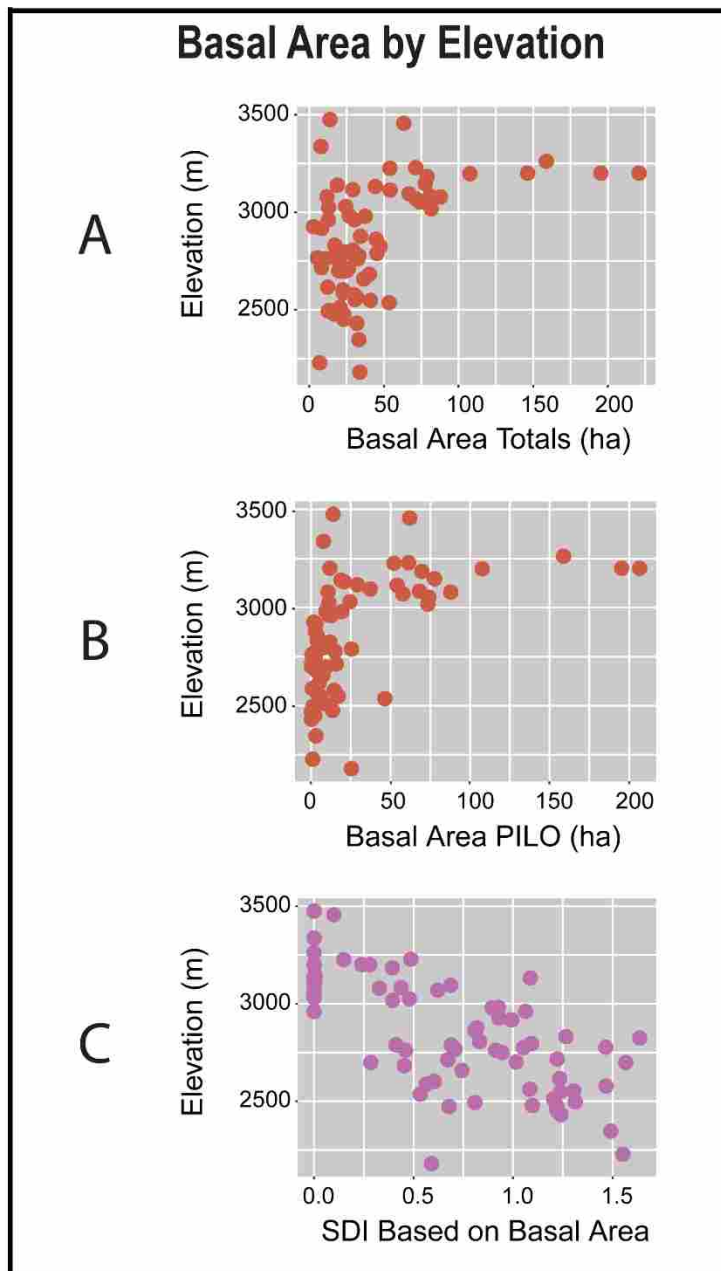


Figure 1 - 5. Scatterplots depict basal area ( $r = 0.466$ ), basal area for PILO ( $r = 0.524$ ), and SDI based on basal area ( $r = -0.691$ ) associations with elevation. Points in each graph represent study plots.

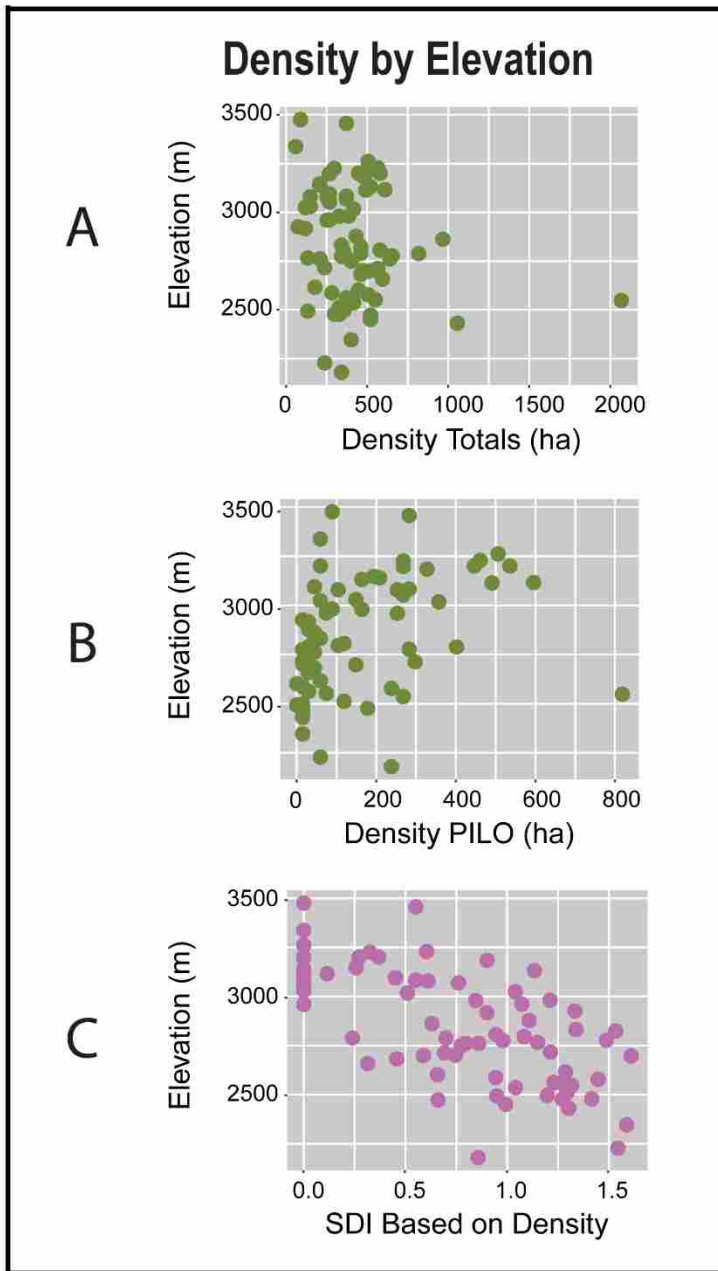


Figure 1 - 6. Scatterplots depict density ( $r = 0.237$ ), density for PILO ( $r = 0.659$ ), and SDI based on density ( $r = -0.658$ ) associations with elevation. Points in each graph represent study plots.

TABLES

Table 1 - 1. Average range values for variables measured at each plot as well as mean values for each variable categorized as either homogeneous or heterogeneous. The t-test p-values are expressed from a two-tailed test. \* Represents statistical significance.

<b>Variable Measured</b>	<b>Range</b>	<b>Homogeneous Plots (expressed as means)</b>	<b>Heterogeneous Plots (expressed as means)</b>	<b>Standard Error</b>	<b>T-test p-value</b>
<b>Biophysical Variables</b>					
Plot elevation	2179 – 3476 (m)	3020 (m)	2662 (m)	55.87 (m)	0.0001*
Plot slope	9 – 112 (degrees)	49 (degrees)	49 (degrees)	5.43 (degrees)	0.8705
Plot aspect	10 – 358 (degrees)	221 (degrees)	195 (degrees)	26.93 (degrees)	0.3285
<b>Stand Composition and Structure</b>					
Tree age	39 – 915 (yrs)	280 (yrs)	212 (yrs)	44.64 (yrs)	0.1320
PILO tree age	34 – 2315 (yrs)	357 (yrs)	282 (yrs)	79.48 (yrs)	0.3477
Tree diameter	13.50 – 72.60 (cm)	371 (cm)	253 (cm)	26.71 (cm)	0.0001*
PILO tree diameter	10.20 – 100.90 (cm)	371 (cm)	253 (cm)	36.39 (cm)	0.0093*
Tree growth rate	1.54 – 22.30 (mm/yr)	1.83 (mm/yr)	1.71 (mm/yr)	0.29 (mm/yr)	0.6971
PILO tree growth rate	1.36 – 22.94 (mm/yr)	1.73 (mm/yr)	1.50 (mm/yr)	0.28 (mm/yr)	0.4225
Plot tree basal area	2.72 – 220.95 (cm/tree)	56.48 (cm/tree)	27.96 (cm/tree)	8.98 (cm/tree)	0.0027*
PILO plot tree basal area	0.12 – 206.60 (cm/tree)	43.62 (cm/tree)	9.74 (cm/tree)	8.98 (cm/tree)	0.0005*
Plot tree density	59.52 – 2068.30 (live trees/hectare)	364 (live trees/hectare)	484 (live trees/hectare)	68.95 (live trees/hectare)	0.0908

PILO plot tree density	14.88 – 818.40 (live trees/hectare)	210 (live trees/hectare)	109 (live trees/hectare)	39.76 (live trees/hectare)	0.0130*
<b>Tree Diversity</b>					
Plot SDI basal area	0 – 1.64	0.37	1.09	0.08	0.0001*
Plot SDI density	0 – 1.61	0.42	1.19	0.07	0.0001*

APPENDIX

Table A - 1. List of study plots by ID, name, and geographic location.

Plot ID	Plot Name	Latitude	Longitude	Elevation (m)
<b>3239</b>	Spring x5	36.344	-115.713	2716.378
<b>3251</b>	Spring x10	36.341	-115.709	3017.520
<b>3252</b>	Spring x6	36.331	-115.638	2795.626
<b>3257</b>	Spring x9	36.318	-115.645	2959.913
<b>3263</b>	Spring x7	36.307	-115.737	2806.294
<b>3265</b>	Spring x15	36.307	-115.581	2430.780
<b>3272</b>	Spring x1	36.303	-115.650	3115.970
<b>3282</b>	Spring x2	36.299	-115.746	2823.972
<b>3284</b>	Spring x13	36.295	-115.680	3113.837
<b>3293</b>	Spring x3	36.285	-115.671	2926.080
<b>3294</b>	Spring x8	36.286	-115.618	2657.856
<b>3295</b>	Spring x4	36.284	-115.609	2877.007
<b>3310</b>	Spring x16	36.262	-115.703	3475.634
<b>3323</b>	Spring x11	36.254	-115.692	3197.657
<b>3324</b>	Spring x14	36.247	-115.610	2698.699
<b>3332</b>	Spring x12	36.242	-115.639	3052.877
<b>52373</b>	White Mtn FIA 2	37.536	-118.197	3261.360
<b>73693</b>	Inyo Mtn	36.960	-118.056	3200.400
<b>80025</b>	N. Schell Creek	39.684	-114.614	2450.897
<b>81219</b>	E. Paragonah	37.857	-112.713	2774.899
<b>81361</b>	W. Emery 1	38.959	-111.318	2562.149
<b>82024</b>	S. Schell Creek	38.916	-114.631	2749.296
<b>82061</b>	E. Joe Valley 2	39.298	-111.179	2227.783
<b>82294</b>	E. Hatch	37.626	-112.363	2346.350

<b>82454</b>	Troy Peak 1	38.325	-115.488	3029.712
<b>82518</b>	Ward	39.076	-114.891	2788.920
<b>82559</b>	Dutton	37.900	-112.248	2917.241
<b>83072</b>	Moriah 1	39.267	-114.099	2862.072
<b>83167</b>	1000 Lake	38.396	-111.521	3079.394
<b>84170</b>	W. Emery 3	38.940	-111.349	2587.142
<b>84663</b>	Cherry 2	40.001	-114.889	2761.488
<b>84806</b>	S. Twisted Forest	37.666	-112.871	2761.488
<b>85420</b>	Lion Mtn	38.172	-111.343	2512.162
<b>85904</b>	S. Wahwah	38.373	-113.575	2496.617
<b>86134</b>	S. Egan	38.834	-114.923	2552.395
<b>86279</b>	Springs 2	36.275	-115.714	2700.833
<b>86472</b>	White Mtn FIA 3	37.790	-118.375	3200.400
<b>86560</b>	S. Snake 1	38.775	-114.187	2831.592
<b>87487</b>	W. Emery 2	38.986	-111.286	2476.500
<b>87529</b>	E. Joes Valley 1	39.329	-111.096	2766.060
<b>87776</b>	Troy Peak 2	38.303	-115.514	3146.450
<b>88149</b>	Hunter Point	39.784	-115.016	2472.842
<b>88638</b>	Bryce Cyn	37.539	-112.242	2616.098
<b>88990</b>	N. White Pine	38.977	-115.444	3024.530
<b>89580</b>	S. Snake 2	38.800	-114.317	2979.725
<b>90338</b>	Moriah 2	39.262	-114.166	3228.746
<b>90503</b>	Cherry 1	39.961	-114.890	2961.132
<b>90566</b>	Lincoln	38.865	-114.296	3337.255
<b>90642</b>	Springs 1	36.364	-115.717	2682.240
<b>90986</b>	White Mtn FIA 1	37.448	-118.181	3078.480
<b>96342</b>	White Mtn FIA 4	37.586	-118.187	3200.400
<b>BAD</b>	Badger	37.557	-118.344	2777.033
<b>BCPT</b>	Bristlecone Point	37.564	-112.852	2980.944



<b>BD</b>	Boundary Peak	37.878	-118.320	3094.634
<b>CV</b>	Cave Mtn	42.134	-114.501	3225.698
<b>EST</b>	East	39.407	-117.202	3183.941
<b>HL</b>	Hill	37.899	-114.583	2788.310
<b>MAM</b>	Mammoth Creek	37.644	-118.673	2577.694
<b>PPT</b>	Powell Point	37.694	-117.899	3131.820
<b>PRC</b>	Price Canyon	39.762	-116.926	2535.936
<b>SOW</b>	Sowers Canyon	39.983	-110.471	2179.625
<b>SPM</b>	Spruce Mtn	40.552	-114.822	3083.052
<b>SWA</b>	Swasey Mtn	39.394	-113.326	2548.128
<b>TF1</b>	Twisted Forest	37.683	-112.881	3069.031
<b>TR1</b>	TR1	37.702	-112.285	2478.024
<b>WAH</b>	Wah Wah	38.595	-113.568	2712.720
<b>WM1</b>	White Mtn 1	37.428	-118.201	3139.440
<b>WM2</b>	White Mtn 2	37.525	-118.195	3456.432
<b>WP</b>	Wilson Point	37.691	-112.307	2697.480

---

Table A - 2. Biophysical variables matrix

<b>Plot Name</b>	<b>Percent Slope</b>	<b>Rock Type 1</b>	<b>Avg Temp</b>	<b>Winter Temp</b>	<b>Summer Temp</b>	<b>Avg Precip</b>	<b>Winter Precip</b>	<b>Summer Precip</b>	<b>sin (Aspect)</b>
3239	15	limestone	5.065417	-0.48333	10.61417	81.30083	129.9167	32.685	-0.25882
3251	60	limestone	5.065417	-0.48333	10.61417	81.30083	129.9167	32.685	0.573576
3252	45	limestone	7.212083	1.505833	12.91833	82.57917	131.8033	33.355	-0.32557
3257	95	limestone	7.212083	1.505833	12.91833	82.57917	131.8033	33.355	-0.17365
3263	65	limestone	6.934583	1.3425	12.52667	77.96	125.1183	30.80167	-0.5
3265	25	limestone	8.820833	3.03	14.61167	44.96083	56.36333	33.55833	0.707106
3272	40	limestone	4.155417	-1.14083	9.451667	87.72084	139.2583	36.18333	0.615661
3282	40	limestone	6.934583	1.3425	12.52667	77.96	125.1183	30.80167	-0.64279
3284	70	limestone	4.155417	-1.14083	9.451667	87.72084	139.2583	36.18333	-0.86603
3293	45	limestone	4.155417	-1.14083	9.451667	87.72084	139.2583	36.18333	0.766046
3294	50	limestone	5.115	-0.42833	10.65833	93.00416	148.3833	37.625	-0.90631
3295	30	limestone	5.115	-0.42833	10.65833	93.00416	148.3833	37.625	0.642787
3310	50	limestone	5.080833	-0.20167	10.36333	94.49166	151.095	37.88833	0.766046
3323	70	limestone	5.080833	-0.20167	10.36333	94.49166	151.095	37.88833	0.642789
3324	55	limestone	7.07625	1.466667	12.68583	96.90833	155.0317	38.785	-0.08716
3332	75	limestone	7.07625	1.466667	12.68583	96.90833	155.0317	38.785	-0.90631
52373	30	sandstone	0.141667	-4.5025	4.785833	79.415	133.8933	24.93667	0.731355
73693	22	sandstone	2.874583	-1.5075	7.256667	51.93583	83.635	20.23667	-0.93969
80025	22	limestone	5.436667	-0.73333	11.60667	72.5325	109.1933	35.87167	0.325568
81219	25	limestone	6.375417	-0.05333	12.80417	72.24083	111.1067	33.375	0.615661
81361	64	shale	5.83625	-0.59	12.2625	66.82917	100.3117	33.34667	-0.3746
82024	90	dolomite	5.268333	-0.8525	11.38917	72.76417	111.3033	34.225	0.173648
82061	70	shale	6.070417	-0.83083	12.97167	65.1425	99.25	31.035	-0.74315
82294	112	sandstone	6.31875	-0.10083	12.73833	71.3675	110.4133	32.32167	-0.74315
82454	73	limestone	4.18125	-1.52667	9.889167	80.2075	122.2567	38.15833	0.99863
82518	74	limestone	6.225	-0.2225	12.6725	70.74167	108.8283	32.655	0.587785
82559	44	ash-flow tuff	4.994167	-1.20833	11.19667	84.1975	128.7583	39.63667	-0.79864
83072	38	limestone	8.616667	1.758333	15.475	53.125	79.84333	26.40667	0.898794

83167	17	alluvium	5.3425	-0.94667	11.63167	65.67417	96.775	34.57333	-0.62932
84170	95	shale	5.83625	-0.59	12.2625	66.82917	100.3117	33.34667	-0.46948
84663	29	dolomite	5.224583	-0.8525	11.30167	76.57167	119.7633	33.38	-0.96126
84806	68	fine-grained mixed clastic	4.345833	-1.55083	10.2425	122.1417	195.275	49.00833	-0.52992
85420	65	sandstone	5.993333	-0.57917	12.56583	62.40333	91.625	33.18167	-0.96592
85904	65	limestone	7.20125	0.720833	13.68167	76.8175	118.7917	34.84333	0.848048
86134	50	dolomite	5.933333	-0.31417	12.18083	67.89667	104.4033	31.39	-0.62932
86279	50	limestone	4.840417	-0.645	10.32583	80.235	127.5767	32.89333	0.766044
86472	63	granodiorite	2.405417	-2.60583	7.416667	60.2625	95.23334	25.29167	-0.76605
86560	60	dolomite	7.71625	1.0375	14.395	64.00083	97.46333	30.53833	0.258819
87487	59	shale	6.34125	-0.3975	13.08	62.30917	94.08166	30.53667	-0.83867
87529	83	shale	6.131667	-0.62	12.88333	67.25917	102.4783	32.04	0.743144
87776	72	limestone	5.27625	-0.73583	11.28833	75.985	116.065	35.905	0.766046
88149	54	dolomite	7.070833	0.526667	13.615	60.80667	92.91167	28.70167	-0.24193
88638	50	limestone	5.614583	-0.7175	11.94667	87.36917	136.445	38.29333	0.984808
88990	65	dolomite	5.7875	-0.4875	12.0625	65.0925	100.15	30.035	0.951056
89580	20	limestone	6.4225	-0.00583	12.85083	70.93083	108.2917	33.57	-0.97029
90338	20	quartzite	4.203333	-1.87417	10.28083	81.66333	126.025	37.30167	-0.90631
90503	51	limestone	6.016667	-0.2975	12.33083	70.34917	109.3217	31.37667	0.978148
90566	15	limestone	2.200417	-3.71417	8.115	111.0158	171.1383	50.89333	0.258821
90642	65	limestone	8.176667	2.418333	13.935	77.87417	125.1983	30.55	-0.86603
90986	10	sandstone	2.29375	-2.40167	6.989167	72.2525	122.595	21.91	0.406739
96342	65	granodiorite	3.179583	-1.6	7.959167	70.9525	119.5067	22.39833	-0.0349
BAD	38	limestone	5.459167	-0.71667	11.635	54.31583	65.37833	43.25333	-0.99939
BCPT	48	fine-grained mixed clastic	2.58375	-3.04	8.2075	139.6817	226.7083	52.655	0.087158
BD	45	diorite	3.367917	-1.59917	8.335	51.76167	81.09333	22.43	-0.0349
CV	25	limestone	3.459167	-2.49917	9.4175	79.6675	122.9783	36.35667	-0.9703
EST	46	alluvium	8.092083	1.515	14.66917	31.6375	45.51667	17.75833	-0.90631
HL	47	limestone	7.670416	1.464167	13.87667	69.3725	109.13	29.615	-0.52992
MAM	39	dacite	5.313334	-0.72833	11.355	47.55083	57.37333	37.72833	0.529921

PPT	9	rhyolite	6.063333	1.0225	11.10417	57.77583	91.595	23.95667	-0.46947
PRC	46	rhyolite	6.97375	0.9425	13.005	68.19167	105.8383	30.545	-0.64279
SOW	65	sandstone	6.38125	-0.99333	13.75583	64.1	96.445	31.755	-0.74315
SPM	65	dolomite	4.150417	-1.73	10.03083	75.66	121.8083	29.51167	-0.93969
SWA	35	limestone	7.922083	1.005833	14.83833	78.74167	120.8033	36.68	-0.97815
WAH	18	limestone	8.985833	2.033333	15.93833	52.45333	78.82333	26.08333	-0.13918
WM1	45	sandstone	4.029167	-0.66333	8.721667	61.935	102.515	21.355	-0.98769
WM2	29	sandstone	0.141667	-4.5025	4.785833	79.415	133.8933	24.93667	0.866026

---

Table A - 3. Growth Rate Matrix

Plot Name	Mean Age	Medium Age	Mean PILO Age	Medium PILO Age	Mean Diameter (mm)	Median Diameter (mm)	Mean Diameter PILO (mm)	Median Diameter PILO (mm)	Mean Growth Rate (Diameter/Age) (mm/yr)	Mean Growth Rate PILO (Diameter/Age) (mm/yr)
3239	86	75	88	88	233.045	207.01	175.26	175.26	2.709826	1.991591
3251	369.75	370.5	411.125	435	462.0986	462.28	474.5567	480.06	1.249759	1.154288
3252	180	177	155.5	155.5	266.4883	226.06	261.2571	180.34	1.480491	1.68011
3257	217.4286	190	217.4286	190	198.2694	172.72	198.2694	172.72	0.911883	0.911883
3263	133.1667	101.5	112.3333	109	199.6831	154.94	243.5225	214.63	1.499497	2.167856
3265	59	60.5	46	46	185.6704	172.72	101.6	101.6	3.146956	2.208696
3272	65.4	58.5	69	62	208.342	182.88	212.7885	185.42	3.185657	3.083891
3282	218.2222	244	375	375	331.7568	287.02	570.6533	589.28	1.52027	1.521742
3284	457.75	364.5	457.75	364.5	332.74	287.02	332.74	287.02	0.726903	0.726903
3293	39	32.5	70	70	185.928	167.64	383.54	383.54	4.767385	5.479143
3294	436.6667	282	535.5	535.5	245.5545	191.77	563.88	563.88	0.562339	1.052997
3295	129	139.5	142	142	270.0283	200.66	331.47	331.47	2.093242	2.334296
3310	680	850	680	850	422.4867	388.62	422.4867	388.62	0.621304	0.621304
3323	256.5455	220	256.5455	220	667.4555	688.34	667.4555	688.34	2.601705	2.601705
3324	139.9167	112.5	36	36	193.6416	166.37	106.68	106.68	1.383978	2.963333
3332	915	974.5	915	974.5	532.9767	593.09	532.9767	593.09	0.582488	0.582488
52373					220.359	242	220.359	242		
73693	161	161	161	161	725.5933	740.41	725.5933	740.41	4.506791	4.506791
80025	147.2222	153	205	205	216.9886	213.36	444.5	444.5	1.473885	2.168293
81219	113.6667	94	300	300	231.5817	218.44	477.52	477.52	2.037376	1.591733
81361	146	146			303.1744	292.1	392.43	392.43	2.076537	
82024	185.3333	165	247.5	247.5	230.4815	215.9	290.83	290.83	1.243605	1.175071
82061	122.375	105.5	84	84	186.5313	184.15	145.415	142.24	1.524259	1.731131
82294	137.0526	118	258	258	269.0519	238.76	508	508	1.963128	1.968992
82454	331	293.5	331	293.5	389.382	331.47	389.382	331.47	1.176381	1.176381
82518	117.2	78.5	199	199	248.5923	223.52	351.79	351.79	2.121094	1.767789

82559	201.4286	119	325	325	273.3675	257.81	505.46	505.46	1.357144	1.555262
83072	138	151.5	156	156	225.8255	210.82	323.4267	320.04	1.636417	2.073248
83167	132.1429	144	165.6	170	295.148	259.08	343.9886	322.58	2.233552	2.077226
84170	169.8182	125	340	340	280.2021	248.92	238.76	238.76	1.650012	0.702235
84663	60.5	57	48	48	224.79	189.23	143.51	143.51	3.715537	2.989792
84806	174.5909	173.5	190.3333	177	231.6126	195.58	220.1333	195.58	1.326601	1.156567
85420	172.5	167.5	187.5	176.5	266.9309	271.78	301.3075	307.34	1.547426	1.606973
85904	96.83333	40.5	207	207	197.5908	185.42	304.8	304.8	2.040525	1.472464
86134	302	340.5	434.3333	434	252.3524	243.84	299.212	307.34	0.835604	0.688899
86279	121.4545	81	284	284	404.9932	137.16	441.96	441.96	3.334525	1.556197
86472	89	89			578.5812	629.92	457.2	457.2	6.500913	
86560	176.7857	183.5	177	181	230.8087	205.74	272.415	255.27	1.305585	1.539068
87487	238.2	230	272.875	250	283.4409	273.05	300.5667	279.4	1.189928	1.101481
87529	58.25	61.5			216.7467	236.22	216.7467	236.22	3.720973	
87776	406.6364	400	444.1	434.5	600.5286	584.2	642.0338	627.38	1.47682	1.445697
88149	80.25	90	86	86	203.708	182.88	139.7	139.7	2.538417	1.624419
88638	203	176.5	213.25	136.5	277.9183	236.22	323.4267	218.44	1.369056	1.516655
88990	53.5	53.5	57	57	303.53	203.2	417.83	356.87	5.673458	7.330351
89580	263.25	279.5	287.4	264	353.8682	340.36	371.5327	355.6	1.344229	1.292737
90338	222.4286	222.5	243.875	244.5	360.8137	340.36	373.9536	340.36	1.622155	1.533382
90503	192.4545	180	191.2	180	351.3667	355.6	415.036	421.64	1.825712	2.17069
90566	305	321	305	321	379.73	346.71	379.73	346.71	1.245016	1.245016
90642	187.2308	187	161.3333	173	288.0852	248.92	274.32	248.92	1.538664	1.700331
90986					620.5071	685.8	620.5071	685.8		
96342					616.0477	594.36	614.68	549.91		
BAD	268.6071	251.5	281.9231	253	213.8218	193.04	224.4558	210.82	0.796039	0.79616
BCPT	222.2308	199	308	308	256.3446	237.49	335.7033	318.77	1.153506	1.089946
BD	513.4444	210	2315	1248.5	445.77	441.96	1009.227	1066.8	0.868195	0.435951
CV	471.6	405	481.7857	407.5	452.755	466.09	473.5689	469.9	0.96004	0.982945
EST	718.5417	419.5	979.9333	1115	395.0494	374.65	467.36	477.52	0.549793	0.47693
HL	211.56	200.5	224.56	161	217.6549	190.5	224.5548	180.34	1.028809	0.999977

MAM	280.25	221	271.8333	160	240.1794	194.31	238.125	171.45	0.857018	0.875996
PPT	166.1515	179	202.1818	198	281.2869	274.32	350.2891	307.34	1.692954	1.732545
PRC	717.6	696.5	801.1176	815	321.7333	284.48	374.1271	345.44	0.448346	0.467006
SOW	662.9048	690	683	751.5	343.5626	342.9	361.1563	337.82	0.518268	0.528779
SPM	438.1176	497	455.1818	515	479.4504	424.18	503.4547	424.18	1.094342	1.106052
SWA	171.8095	154	184.1633	169	134.6381	111.76	139.6093	125.73	0.783648	0.758073
WAH	204.6053	178	256.15	191.5	210.4858	204.47	238.887	232.41	1.028741	0.932606
WM1	225.5	233	225.5	233	310.2429	281.94	310.2429	281.94	1.3758	1.3758
WM2	246.7778	145	310.5385	145	375.1072	330.2	455.5958	386.08	1.52002	1.467115

---

Table A - 4. Stand Structure Matrix

Plot Name	LTD: Total (ha)	LD: propor PILO	Shannon's DI	spec rich-ness	Basal_Area_Totals	Shannon's DI 2	LBA propor PILO
3239	238.08	0.0625	1.212314	4	8.062552	1.222261	0.044523
3251	416.64	0.857143	0.509137	3	81.61852	0.394693	0.899073
3252	357.12	0.291667	1.083529	3	23.85236	1.093475	0.312987
3257	252.96	1	0	1	12.70346	0	1
3263	580.32	0.205128	0.944891	4	29.16582	0.831704	0.214374
3265	1056.48	0.014085	1.302029	6	31.82014	1.241145	0.003791
3272	610.08	0.97561	0.114665	2	29.13151	0.003315	0.999627
3282	461.28	0.096774	1.532985	7	47.39054	1.636857	0.248685
3284	491.04	1	0	1	54.05393	0	1
3293	74.4	0.2	1.332179	4	2.719009	0.929134	0.632272
3294	595.2	0.05	0.314123	3	36.41543	0.743574	0.208595
3295	431.52	0.068966	1.107891	5	34.27548	0.818848	0.07585
3310	89.28	1	0	1	13.81355	0	1
3323	267.84	1	0	1	107.6307	0	1
3324	565.44	0.052632	0.587926	3	19.6891	0.285327	0.015471
3332	267.84	1	0	1	74.00519	0	1
52373	505.92	1	0	1	158.7677	0	1
73693	446.4	1	0	1	195.3164	0	1
80025	520.8	0.028571	0.991533	5	23.10064	1.221578	0.099957
81219	342.24	0.043478	0.979238	4	17.0859	1.052066	0.155969
81361	372	0.08	1.229344	5	31.75861	1.084339	0.121518
82024	401.76	0.074074	0.774311	3	19.77694	0.945327	0.130709
82061	238.08	0.25	1.543789	5	6.932334	1.552124	0.143665
82294	401.76	0.037037	1.586884	7	33.17987	1.490775	0.090896
82454	148.8	1	0	1	24.38912	0	1
82518	461.28	0.064516	0.239217	2	27.9685	0.411741	0.143766
82559	119.04	0.25	0.900256	3	8.225714	0.992736	0.362989
83072	967.2	0.046154	0.630436	4	44.77483	0.807428	0.081968



83167	148.8	0.7	0.610864	2	11.84581	0.328801	0.898301
84170	282.72	0.052632	0.943046	4	22.64147	0.563297	0.029425
84663	208.32	0.142857	0.796312	3	10.53094	0.46016	0.046001
84806	639.84	0.069767	0.86006	4	32.52157	0.911603	0.059087
85420	327.36	0.363636	1.294545	4	20.55414	1.203916	0.415699
85904	357.12	0.041667	1.196711	6	13.53148	1.312928	0.080238
86134	550.56	0.135135	1.275903	5	30.54063	1.30523	0.175296
86279	476.16	0.03125	0.746241	4	25.09153	1.014793	0.090977
86472	491.04	0.121212	0.369333	2	146.2722	0.279987	0.080499
86560	342.24	0.173913	1.337787	4	16.98585	1.266009	0.223848
87487	327.36	0.545455	1.270761	5	23.11655	1.21873	0.583118
87529	133.92	0.222222	1.14906	4	5.383354	0.709188	0.427919
87776	208.32	0.928571	0.257319	2	77.67142	0.004746	0.999441
88149	520.8	0.028571	0.659747	3	20.51803	0.678129	0.011116
88638	178.56	0.333333	1.286057	4	12.30641	1.23429	0.401559
88990	119.04	0.5	1.039721	3	12.86594	0.478769	0.868952
89580	327.36	0.5	0.845465	3	37.45894	0.89475	0.515679
90338	565.44	0.815789	0.603517	3	71.25549	0.486326	0.860463
90503	267.84	0.277778	1.072043	3	30.41426	1.062605	0.367609
90566	59.52	1	0	1	7.796321	0	1
90642	461.28	0.096774	0.457102	3	40.22824	0.45299	0.069947
90986	252.96	1	0	1	87.82024	0	1
96342	580.32	0.923077	0.271189	2	220.9455	0.239793	0.935268
BAD	654.72	0.431818	1.487605	5	33.20249	1.465812	0.450868
BCPT	386.88	0.230769	1.210307	5	26.83391	0.926132	0.349616
BD	267.84	0.166667	0.450561	2	66.82841	0.686954	0.55559
CV	297.6	0.9	0.325083	2	53.97762	0.14984	0.965564
EST	476.16	0.6875	0.901694	4	78.92854	0.392936	0.882929
HL	818.4	0.490909	0.69856	3	45.30035	0.689258	0.560227
MAM	505.92	0.470588	1.446593	6	29.82412	1.46651	0.483973
PPT	520.8	0.314286	1.13305	5	44.26114	1.086637	0.469281

PRC	416.64	0.642857	1.040649	5	53.42233	0.533828	0.868365
SOW	342.24	0.695652	0.856859	4	33.87368	0.590169	0.747787
SPM	372	0.76	0.55108	2	81.0338	0.437937	0.841042
SWA	2068.32	0.395683	1.316432	4	40.87855	1.237554	0.417475
WAH	565.44	0.526316	0.691761	2	26.20923	0.672057	0.602326
WM1	208.32	1	0	1	18.76329	0	1
WM2	372	0.76	0.55108	2	63.29737	0.099472	0.979631

---

## CHAPTER 2

### A Comprehensive Distribution Map of Great Basin

#### Bristlecone Pine (*Pinus longaeva*)

Gregory W. Taylor<sup>1</sup>, Stanley G. Kitchen<sup>2</sup>, Douglas H. Page<sup>2</sup>, David A. Charlet<sup>3</sup>, Steven L. Petersen<sup>1</sup>

<sup>1</sup>Department of Wildlife Sciences, Brigham Young University, Provo, UT 84602

<sup>2</sup>US Forest Service, Rocky Mountain Research Station, Provo, UT 84606

<sup>3</sup>Department of Biology, College of Southern Nevada, Las Vegas, NV 89002

#### ABSTRACT

The physical mapping of forests allows for a greater view into ecological effects that may be affecting the health of these forests over time. Mapping forest communities has become more time efficient and accurate through the application of geographic information systems (GIS) and remote sensing technology. Researchers and managers are able to effectively apply these tools to characterize forest communities and accurately delineate specific features (e.g. tree stands, individual plants, natural and anthropogenic disturbances) over large geographical spaces. Combining remotely sensed imagery with GIS image processing software, scientists can identify unique spectral, spatial, and temporal characteristics that improve object identification and classification. In this study we developed a comprehensive, digital map of the current distribution of *Pinus longaeva* using all available information in the form of herbarium records, USDA Forest Service unpublished records, published records, and on-site visitations. Using remotely sensed imagery, GIS programs ArcMAP and QGIS, and electronic records we mapped 678 unique stands (polygons) totaling 121,121 ha widely distributed across the southern and central Great Basin and clustered along the western rim of the Colorado Plateau. These stands span 42 mountain ranges from the White Mountains on the western edge of the Great Basin to

the Colorado Plateau's Henry Mountain and West Tavaputs Plateau in the East, and from the Spring Mountains in the South to the Ruby and Spruce Mountains in the North. Stands were separated into four general sub-regions: Western Great Basin, Southern Great Basin, Central Great Basin, and Colorado Plateau. We compared the number of polygons, the average polygon size, and total hectares in the *P. longaeva* distribution in each sub-region. Mapping accuracy was evaluated by assessing polygon overlap between the subset of our polygons located within the state of Nevada (231 polygons) with an independently developed control set of maps for the state (63 polygons). Of the total area mapped (72,336 ha), 32% (23,235 ha) was included in both efforts with the majority of the remainder (43,459 ha) not included in the control data set suggesting that our effort was either more thorough, more speculative, or both. Not only did the polygons differ in shape and size between maps, but there were also 60 polygons (mean polygon size = 70 ha) that we mapped in different areas that the control set did not include. Also there were 11 polygons (mean polygon size = 184 ha) that we did not include that were included in the control set. Knowing where *P. longaeva* occurs is important for management implications because it allows forest managers to monitor temporal and spatial changes in stands over time. Monitoring is required because of forest changes due to natural and anthropogenic hazards. In order for forest managers to respond to risk and to minimize changes, accurate and detailed inventories are necessary. Knowledge of species location also provides a better foundation to plan and design future studies across the entire *P. longaeva* distribution.

## INTRODUCTION

Initially, geographic information systems (GIS) and remote sensing tools were useful tools for mapping specific areas of interest and understanding spatial patterns; however GIS and

remote sensing tools have since become highly utilized for characterizing forest communities by detecting spatial, spectral, and temporal differences and similarities between plants or other structures (Xie et al. 2008), detecting temporal changes in landscapes over time (Brink and Eva 2009), monitoring poaching (Jachmann 2008, Mulero-Pázmány et al. 2014), and improving crop yield (Moran et al. 1997). Recent advancements in remote sensing through light detection and ranging (LIDAR) allow researchers to visualize forest structure by modeling forest topography and infrastructure and predicting forest volume and biomass (Kelly and Di Tommaso 2015). The broad applicability and incorporation of remote sensing and GIS are being used with more frequency across a greater spectrum of fields. In this study we use both remote sensing techniques and GIS tools to map the distribution of *Pinus longaeva* D.K. Bailey (Great Basin bristlecone pine).

During the late Pleistocene (30–12 k.y.a.) *Pinus longaeva* was one of the most widespread and dominant tree species in the southern Great Basin ecoregion (LaMarche 1973). Packrat midden records suggest that it was common to as low as 1,800 meters in elevation, however, due to the warmer and drier climate of the Holocene, *P. longaeva* receded to higher elevations where it is most commonly associated with wind-swept mountain peaks, limestone precipices, and locations subjected to below freezing mean annual temperatures (Betancourt et al. 1990). This retreat resulted in high dis-connectivity among stands in the Great Basin. A knowledge of the spatial distribution of Great Basin bristlecone pine and what variables influence that distribution will provide insight into its present and projected future occurrence.

The objectives of our study were to create an accurate and complete digital distribution map for *P. longaeva* using all sources of available data and to evaluate accuracy of the map and associated methods by comparing our mapped polygons to a control set of maps developed

independently for the state of Nevada. An accurate and robust mapping of *P. longaeva* allows forest researchers unprecedented insight into the lifecycle of the species. By understanding the distribution of the species and its change over time, we can get a view into ecological effects that may be affecting the health of *P. longaeva*. We can see the effect of fire on the species, and even possibly be able to see the impact of climate change on favorable habitats over time.

## METHODS

### *Mapping*

We developed a comprehensive distribution map for GBBP using Geographic Information Systems (GIS) software in association with remotely sensed imagery (Figures 2-1 and 2-2). Broad and precise locations of *Pinus longaeva* stands were first identified from previous maps (US Forest Inventory and Analysis plot information and USDA Forest Service agency herbarium and other electronic records (Charlet 2015), local expertise, and site visitations. Using these tools as a general reference to identify *P. longaeva* stands we then focused on specific stands through remotely sensed imagery (65 cm spatial imagery from Google Earth and Bing Imagery) (Figure 2-2). In areas where the conditions appeared suitable for *P. longaeva* growth, we performed on site visitations to those locations to identify stands. On steep slopes and rough terrain, we used remote sensing to identify *P. longaeva* stands (It should be known that remote sensing has its limitations, which will be discussed in more detail in the discussion.) Once stands were identified, the area extent around the stands were defined using ArcMAP v. 10.5. We used polygons to demarcate stands and points to mark individual trees that were not thought to be associated with a distinct stand (Figure 2-1). We accomplished this by defining the area extent around confirmed GBBP stands in ArcMAP.

To provide an opportunity for a more in depth analysis across the full *P. longaeva* range, we assigned stands into four distinct geographical sub-regions: These are: western Great Basin, southern Great Basin, Central Great Basin and Colorado Plateau (Figure 2-1). The Western Great Basin sub-region includes all stands in the White, Inyo, Panamint and Silver Peak Mountain ranges in eastern California and western Nevada. The Southern Great Basin sub-region includes stands in the Spring Mountains, Potosi Mountain, and the Sheep Range in southern Nevada. The Colorado Plateau sub-region includes all stands in the High Plateaus and Mountains of Central and Southern Utah that form the western margins of the Colorado Plateau. The Central Great Basin sub-region includes all stands found on the numerous, mostly north and south trending ranges of the Great Basin interior and located in western Utah and central Nevada. These sub-regions were identified and labeled based on geographical representation and differences in geology (Bailey 1970, Bailey 1980). The polygons included in the Western Great Basin and Southern Great Basin sub-regions appear on older and more calcareous surfaces than the other two sub-regions (Fiero 2009).

To validate our efforts, we compared total number of polygon and their associated areas as well as polygons >1000 ha for the Nevada portion of our completed map with those compiled for the control set of maps for that state (Charlet 2015). We checked both the total number of polygons and only the polygons >1000 ha to see if there was a significant difference in percent overlap. We identified specific polygons included in both mapping efforts and those that were unique to one or the other. We quantified the area of agreement as a percentage of the total area mapped between the two efforts. We also quantified the area that was unique to the separate efforts.

## RESULTS

### *Mapping*

We mapped a total of 113,886 ha in 685 unique stands (polygons) on 42 mountain ranges across the full range of the species distribution (Figures 2-2 and 2-3). Stands ranged in size from 1 to 15,644 ha. Largest continuous stands (> 1,000 ha) were found on the White Mountains, the Sheep Range, the Spring Mountains, the Snake Range, the Grant Range, the Ruby Mountains, the Escalante Mountains, and the Markagunt and Paunsaugunt Plateaus. These larger areas of occurrence are spread somewhat evenly east to west. Differences in number of polygons, mean polygon size, and total hectares by sub-region can be found in Table 2-1. Polygon sizes were overall larger in the Western and Southern Great Basin sub-regions in comparison to the Central Great Basin and Colorado Plateau sub-regions whose polygons were smaller and more numerous.

We found a 36% overlap (23,235 of 65,101 ha) between the two mapping efforts (Figure 2-4). The control data set identified 5,642 hectares that were not included in our assessment, while we mapped 36,224 hectares that were not in the control set. Overall our map identified a total of 229 distinct *P. longaeva* stands (average polygon size = 289 ha) while the control map identified 63 (average polygon size = 458 ha). Additionally, we mapped 59 unique stands (mean polygon size = 70 ha) that the control map did not, and the control map identified 11 stands (mean polygon size = 184 ha) that we did not. We ran the analysis again to determine percent overlap between polygons >1000 ha for the two maps. We found a 20% overlap (8,648 of 43,412 ha) between the two mapping efforts. Our map identified 9 polygons with an average polygon size of 3,816 ha while the control map identified 8 polygons with an average polygon size of



2,214 ha. We did not find a significant percent overlap difference between total number of polygons and only polygons >1000 ha ( $p = 0.56$ ).

## DISCUSSION

*Pinus longaeva* is currently found in the Colorado Plateau and Great Basin. Across the four sub-regions we observed that the largest polygons were found on the White Mountains and Spring Mountains. Areas with the most polygons were found mainly in the Central Great Basin and Colorado Plateau. It is interesting to note that there were many locations with suitable habitat where we expected to find *P. longaeva* but we did not (e.g. the area between the central Great Basin and Western Great Basin, areas within the Central Great Basin and the Colorado Plateau, and it is not present in the Wasatch Mountains). We speculate that this is largely due to differences in soil type, given that the other environmental conditions (e.g. precipitation, temperature, elevation) do not change much across the *P. longaeva* distribution. This occurred in the Colorado Plateau where limestone soils dominate most of the region, but *P. longaeva* stands were spread out on mostly North-western and north-eastern aspects. This also occurs in the Central Great Basin where soils are predominately sandstone/limestone based, but the *P. longaeva* stands seem to be correlated with elevations above 2316 m on north-eastern and north-western aspects. Vary rarely did we find *P. longaeva* stands on southern aspects except at the highest elevations where *P. longaeva* grew mostly independent of aspect (White Mountains, Snake Range, Spring Mountains).

We believe that the *P. longaeva* stands are larger in both the Western and Southern Great Basin because the habitat is more suitable in those areas and the mountain ranges within those regions have more area (ha) at higher elevations. As *P. longaeva* is the dominant tree species in these areas we mapped, more available space at higher elevations provides greater space for

growth, which results in greater tree coverage and larger polygons within these sub-regions.

Despite the larger polygon sizes in those two sub-regions, the total number of hectares mapped were similar between the larger and smaller polygons.

We found that *P. longaeva* distribution is more widespread in the Colorado Plateau than US Forest Service maps indicated, and more widespread in Nevada than indicated by the control map (Charlet 2015). The polygons that overlapped most frequently tended to be the larger polygons that encompassed areas where *P. longaeva* does not co-exist with several other species (White Mountains). Additionally, our mapping efforts proved to overestimate *P. longaeva* stand sizes in comparison with the control map. Due to the textural similarities between *P. flexilis* and *P. longaeva* and our clear bias to not miss any possible *P. longaeva* trees, it is possible that we may have overestimated the *P. longaeva* distribution, but it also could mean that we were able to identify areas that were not previously identified by the control map. Despite our efforts to not exclude any *P. longaeva* stands, we acknowledge that some stands may have been left out of the mapping effort due to those same difficulties mentioned previously. It is also possible that both our map and the control map either excluded or included *P. longaeva* stands and individuals across the geographic distribution. These errors of omission and commission cannot be pinpointed on one map or the other due to there not being a completely accurate *P. longaeva* distribution map to which we can compare.

Despite unknown errors of omission and commission we feel confident that this map represents the most complete and accurate map of *P. longaeva* available to date. The only other map with which we can compare our map is the control map, which only includes *P. longaeva* stands within the state of Nevada (Charlet 2015). All other maps focused on stands located in the Snake Range, Markagunt Plateau, Paunsaugunt Plateau, White Mountains, Spring

Mountains, Cherry Creek Range, and Schell Creek Range, Deep Creek Range, Tushar Mountains (Currey 1965, Wright and Mooney 1965, LaMarche 1969, Nelson 1976, Beasley and Klemmedson 1980, Hiebert and Hamrick 1984, Orlemann 2017). This map includes every known population of *P. longaeva* across its distribution.

As technology improves, the techniques for mapping are also changing. One of the current challenges in comparing different maps is the different techniques for data collection. As satellite imagery improves, it will increasingly be possible to refine maps without physically being on the ground. Clearly, these data collection techniques will not exactly match maps that were created while physically walking around the area of interest. The benefit of remote mapping, however, is that we can update the information more frequently than previously possible. This increased frequency will allow researchers to react to changes, adaption, and even ecological disasters in the making. Knowing where *P. longaeva* occurs is important for management implications because it provides forest managers with a comprehensive knowledge of where each *P. longaeva* population is found and allows them to monitor temporal and spatial changes in stands over time. It also provides them with a better foundation to plan and design future studies across the entire *P. longaeva* distribution.

#### ACKNOWLEDGMENTS

This project was partially funded by a grant from the USDA Forest Service, Western Wildland Environmental Threat Assessment Center and the Rocky Mountain Research Station (RJVA-14-JV-11221632-099). Additional funding was also provided by Brigham Young University, Charles Redd Foundation Center for Western Studies. We appreciate the support and resources provided by the Brigham Young University Geospatial Habitat Analysis Laboratory.

We especially thank Teresa Gomez for her geospatial expertise and Michael Witt for helping identify *P. longaeva* stands in the field.

## LITERATURE CITED

- Bailey, D. K. 1970. Phytogeography and taxonomy of pinus subsection Balfourianae. *Annals of the Missouri Botanical Garden* 57:210-249.
- Bailey, R. G. 1980. Description of the ecoregions of the United States. US Department of Agriculture, Forest Service.
- Beasley, R. S., and J. O. Klemmedson. 1980. Ecological relationships of bristlecone pine. *The American Midland Naturalist* 104:242-252.
- Betancourt, J. L., T. R. Van Devender, and P. S. Martin. 1990. Packrat middens: the last 40,000 years of biotic change. University of Arizona Press.
- Brink, A. B., and H. D. Eva. 2009. Monitoring 25 years of land cover change dynamics in Africa: A sample based remote sensing approach. *Applied Geography* 29:501-512.
- Charlet, D. A. 2015. Atlas of Nevada Conifers: a phytogeographic reference. Second edition. University of Nevada, Reno, Nevada. Unpublished data.
- Currey, D. R. 1965. An ancient bristlecone pine stand in Eastern Nevada. *Ecology* 46:564-566.
- Fiero, B. 2009. Geology of the Great Basin. University of Nevada Press, United States of America.
- Hiebert, R. D., and J. L. Hamrick. 1984. An ecological study of bristlecone pine (*Pinus longaeva*) in Utah and Eastern Nevada. *Great Basin Naturalist* 44:487-494.
- Jachmann, H. 2008. Monitoring law-enforcement performance in nine protected areas in Ghana. *Biological Conservation* 141:89-99.
- Kelly, M., and S. Di Tommaso. 2015. Mapping forests with Lidar provides flexible, accurate data with many uses. *California Agriculture* 69:14-20.
- LaMarche, V. C. 1969. Environment in relation to age of bristlecone pines. *Ecology* 50:53-59.

- LaMarche, V. C. 1973. Holocene climatic variations inferred from treeline fluctuations in the White Mountains, California. *Quaternary Research* 3:632-660.
- Moran, M. S., Y. Inoue, and E. M. Barnes. 1997. Opportunities and limitations for image-based remote sensing in precision crop management. *Remote Sensing of Environment* 61:319-346.
- Mulero-Pázmány, M., R. Stolper, L. D. van Essen, J. J. Negro, and T. Sassen. 2014. Remotely piloted aircraft systems as a rhinoceros anti-poaching tool in Africa. *PLOS ONE* 9:e83873.
- Nelson, M. G. 1976. The montane coniferous forests of the northern Deep Creek Range, Utah. Unpublished thesis, University of Utah, Salt Lake City:73.
- Orlemann, A., Flinders, Steven H., Allphin, Loreen. 2017. The discovery of Great Basin bristlecone pine, *Pinus longaeva*, in the Tushar Mountains of the Fishlake National Forest in Central Utah, USA. *Western North American Naturalist* 77:7.
- Weigle, W. G., and E. H. Frothingham. 1911. The aspens: their growth and management. U. S. Department of Agriculture Forest Service - Bulletin 93:1-34.
- Wright, R. D., and H. A. Mooney. 1965. Substrate-oriented distribution of bristlecone pine in the White Mountains of California. *The American Midland Naturalist* 73:257-284.
- Xie, Y., Z. Sha, and M. Yu. 2008. Remote sensing imagery in vegetation mapping: a review. *Journal of Plant Ecology* 1:9-23.

## FIGURES

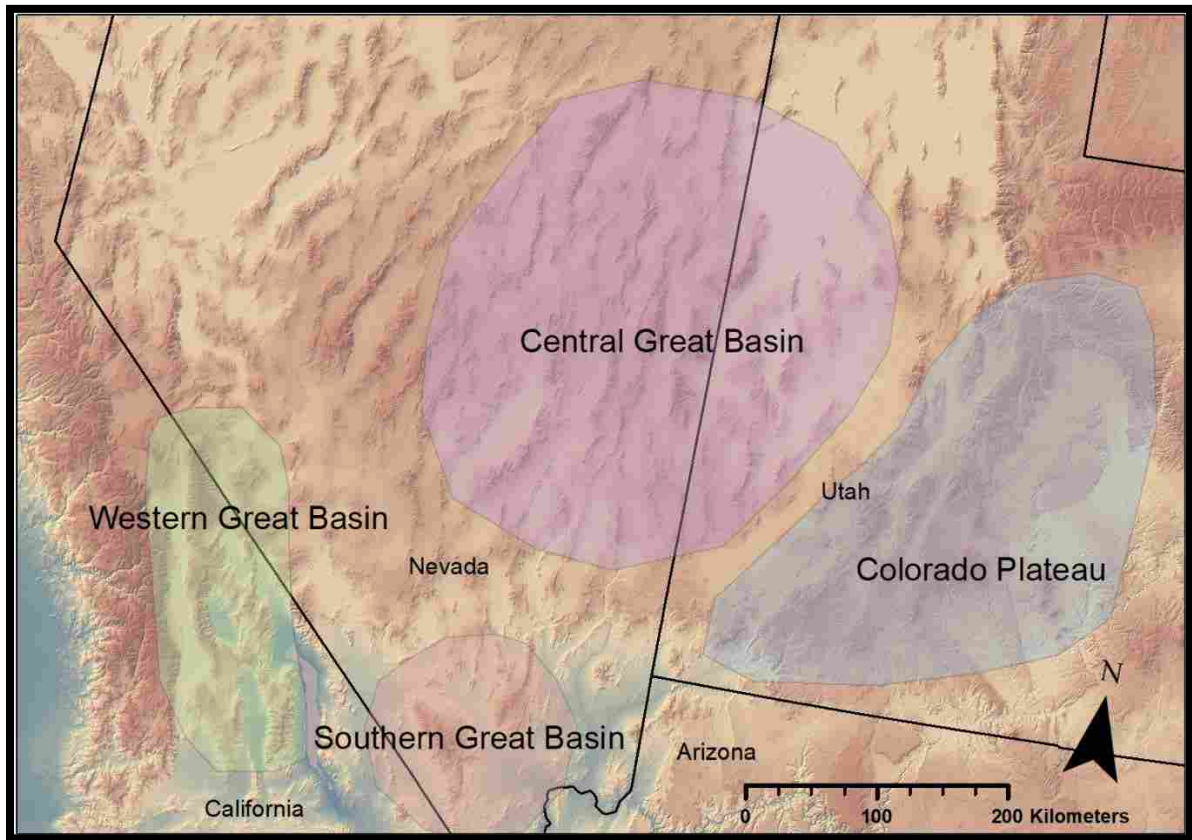


Figure 2 - 1. The four distinct geographical sub-regions where *Pinus longaeva* stands were assigned.

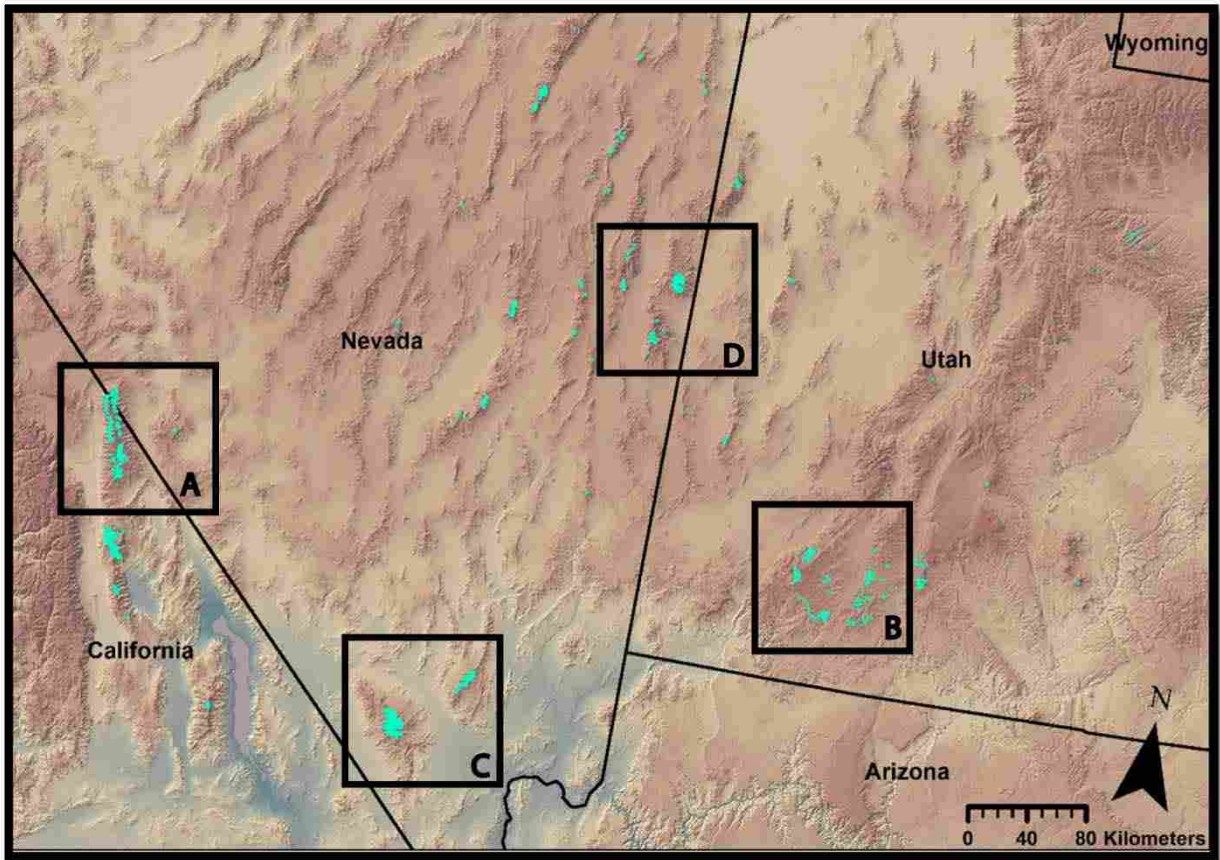


Figure 2 - 2. Comprehensive *Pinus longaeva* distribution map. Teal polygons represent current *Pinus longaeva* stands. Boxes delineate areas seen at higher resolution in figure 2–2.



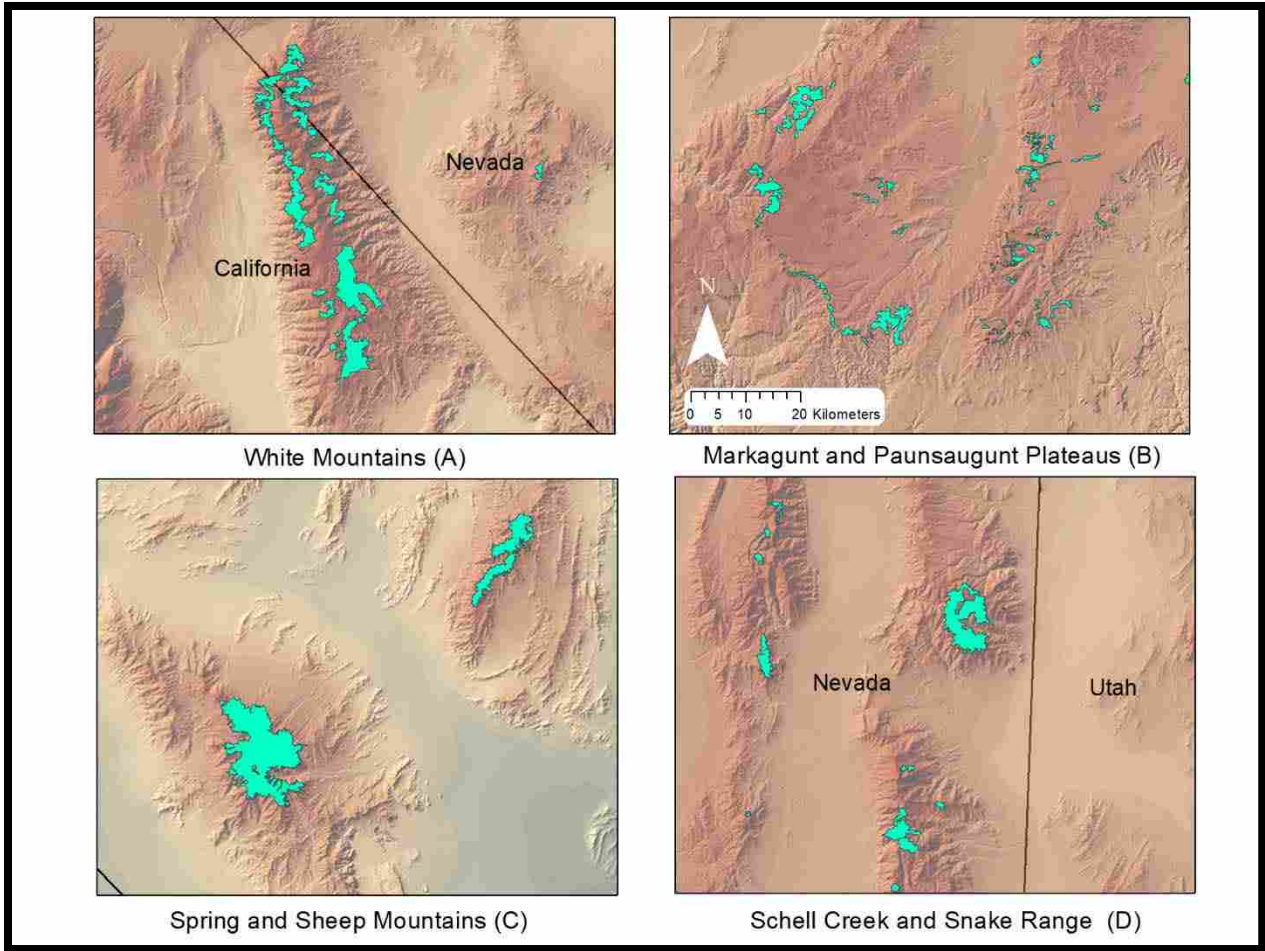


Figure 2 - 3. Select localities depicting *Pinus longaeva* distribution map. Teal polygons represent current *P. longaeva* stands.

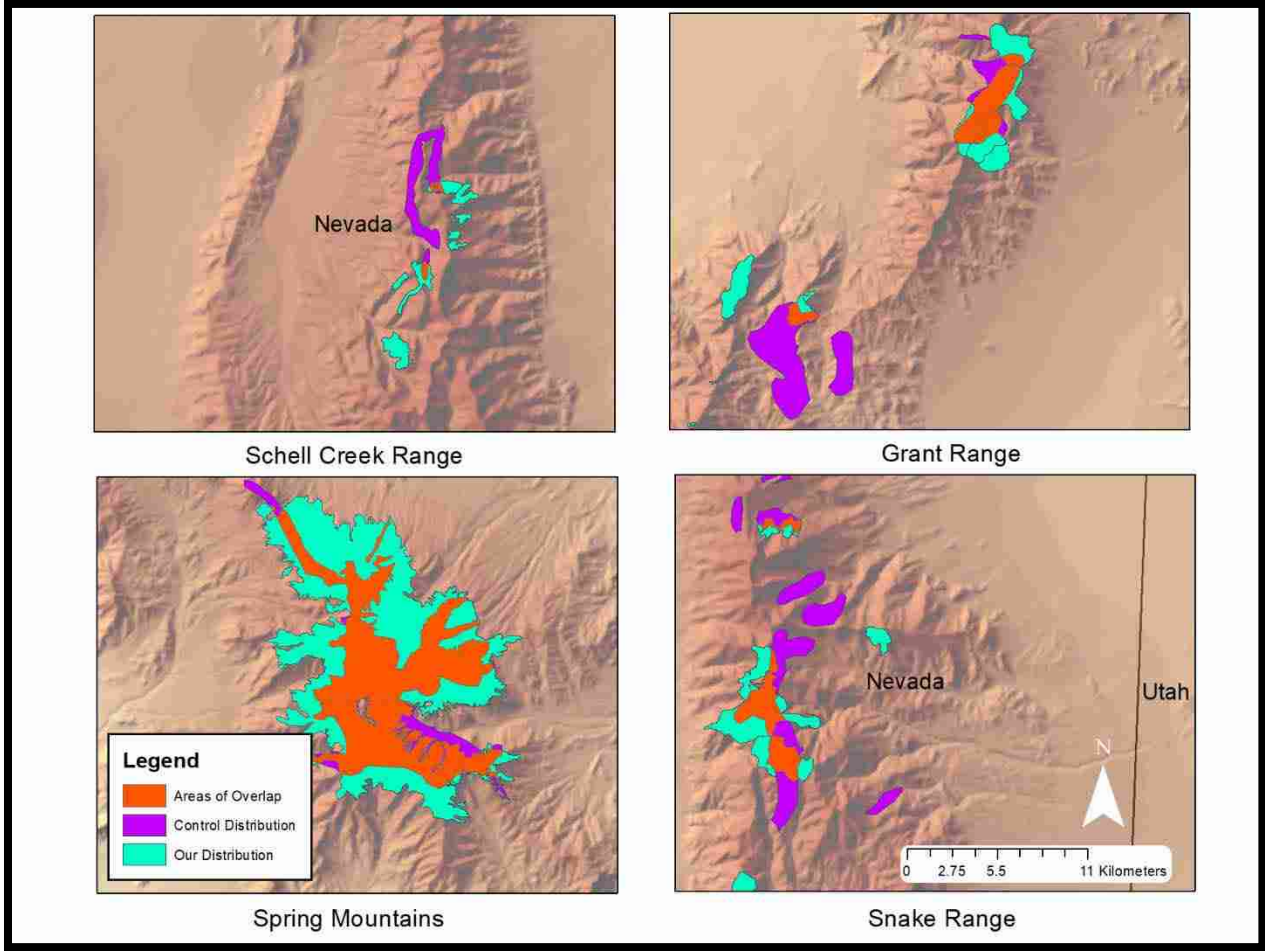


Figure 2 - 4. Comparison between the control *Pinus longaeva* distribution map (purple polygons) and our map (teal polygons) at select localities in the state of Nevada. The fire orange polygons demonstrate the areas of overlap between the control distribution and ours.

## TABLES

Table 2 - 1. Number of polygons and total hectares found in each of the four *P. Longaeva* sub-regions.

<b>Sub-region</b>	<b>Number of Polygons</b>	<b>Mean Polygon Size (ha)</b>	<b>Total Area (ha)</b>
Western Great Basin	45	780	35,086
Southern Great Basin	4	5096	20,385
Central Great Basin	299	61	38,152
Colorado Plateau	334	151	20,237

APPENDIX

Table A - 5. List of Mountain ranges where *Pinus longaeva* is found across the four sub-regions.

<b>Sub-region</b>	<b>Mountain Ranges</b>
Western Great Basin	Inyo Mountains
	White Mountains
	Panamint Peak
	Silver Peak
Southern Great Basin	Sheep Range
	Spring Mountains
	Potosi Mountain
Central Great Basin	Cherry Creek Range
	Egan Range
	Fish Creek Range
	Hot Creek Range
	Monitor Range
	Mountain Home Range
	Quinn Canyon Range
	Schell Creek Range
	Seaman Range
	Snake Range
	Toiyabe Range
	Deep Creek Mountains
	Goshute Mountains
	Ruby Mountains
	Wah Wah Mountains
Currant Mountain	
Sherman Mountain	

Spruce Mountain  
Summit Mountain  
Frisco Peak  
Highland Peak  
Swasey Peak  
Troy Peak

---

Colorado Plateau

Markagunt Plateau  
Old Woman Plateau  
Pahvant Plateau  
Paunsaugunt Plateau  
Sevier Plateau  
Wasatch Plateau  
West Tavaputs Plateau  
Escalante Mountains  
Henry Mountains  
Pine Valley Mountains  
Tushar Mountains  
Mount Dutton

---